VOL 10
ISSUE 4
July 2025

eMetN METEOR JOURNAL

eJournal for meteor observers **www.emetn.net**

Fireball of at least -8 over Belgium, 2025 June 27, 23h59m32s UT, recorded by 16 Global Meteor Network cameras in Belgium, France, the Netherlands and the United Kingdom. This All-sky photo was obtained by Franky Dubois at Langemark, Belgium.

ISSN 3041 - 4261

Contents

New version of the orbital IAU Meteor Data Center database (Version 2025)

L. Neslušan, M. Jakubík

Astronomical Institute of the Slovak Academy of Sciences, Tatranská Lomnica, Slovakia
ne@ta3.sk, mjakubik@ta3.sk

On April 2025, the IAU Meteor Data Center team, part of orbital database, issued the new version of the orbital database, Version 2025. Its content considerably increased. The video EDMOND, GMN, and radio AMOR data are included.

Announcement

The IAU Meteor Data Center (MDC) is a central repository of the orbital and other data of individual meteors (MO part of the MDC) and the official database of known meteor showers (SD part). We announce that the orbital database was recently enlarged including: 2001–2017 EDMOND (European viDeo MeteOr Network Database) (Kornoš et al., 2014a; Kornoš et al., 2014b), 2018–2024 GMN (Global Meteor Network) (Vida et al., 2020; Vida et al., 2021), 2024 SonotaCo (SonotaCo et al., 2021), and 1990–1999 AMOR (Advanced Meteor Orbit Radar) (Baggaley, 1983; Baggaley et al., 1993; Baggaley, 1996; Baggaley, 1999) data.

The new - Version 2025 - IAU MDC database contains:

- 6345 - photographic meteor orbits (42 individual catalogs);
- 3206547 - video meteor orbits (5 catalogs);
- 11937769 - radar meteor orbits (3 catalogs).

The IAU MDC public-domain data can be downloaded, all catalogs in the same format, from the MDC site[1]:

The orbital part is accessible online[2].

References

Baggaley J.W. (1983). "The determination of meteoroid orbits by radar". *Southern Stars*, **30**, 285–289.

Baggaley J. W., Taylor A. D., Steel D. I. (1993). "The Southern Hemisphere Meteor Orbit Radar Facility: AMOR". In *Meteoroids and Their Parent Bodies*, eds. J. Štohl and I. P. Williams, Astron. Inst., Slovak Acad. Sci., Bratislava, pp. 245–248.

Baggaley J. W., Bennett R. G. T. (1996). "The Meteoroid Orbit Facility Amor: Recent Developments". In *Physics; chemistry; and dynamics of interplanetary dust*, Astronomical Society of the Pacific Conference Series; Proceedings of the 150th colloquium of the International Astronomical Union (ASP 104), eds. B. A. S. Gustafson and M. S. Hanner, Astronomical Society of the Pacific, San Francisco, p. 65.

Baggaley J. W. (1999). "Using the AMOR radar facility to probe the atmosphere". In *Meteoroids 1998*, eds. W. J. Baggaley and V. Porubčan, Astron. Inst., Slovak Acad. Sci., Bratislava, pp. 15–20.

Kornoš L., Koukal J., Piffl R., and Tóth J. (2014a). "EDMOND Meteor Database". In *Proc. International Meteor Conference 2014*, eds. M. Gyssens, P. Roggemans, P. Zoladek, International Meteor Organization, pp. 23–25.

Kornoš L., Matlovič P., Rudawska R., Tóth J., Hajduková M. Jr., Koukal J., Piffl R. (2014b). "Confirmation and characterization of IAU temporary meteor showers in EDMOND database". In *Proc. Meteoroids 2013 Conference*, eds. T. J. Jopek, F. J. M. Rietmeijer, J. Watanabe, I. P. Williams, A. M. University Press, Poznań, pp. 225–233.

SonotaCo, Masuzawa T., Sekiguchi T., Miyoshi T., Fujiwara Y., Maeda K., Uehara S. (2021). "Ongoing Meteor Network. SNMv3: A Meteor Data Set for Meteor Shower Analysis". *WGN, Journal of the International Meteor Organization*, **49**, 64–70.

Vida D., Gural P. S., Brown P. G., Campbell-Brown M., Wiegert P. (2020). "Estimating trajectories of meteors: an observational Monte Carlo approach - I. Theory". *Monthly Notices of the Royal Astronomical Society*, **491**, 2688–2705.

Vida D., Šegon D., Gural P. S., Brown P. G., McIntyre M. J. M., Dijkema T. J., Pavletić L., Kukić P., Mazur M. J., Eschman P., Roggemans P., Merlak A., Zubović D. (2021). "The Global Meteor Network - Methodology and first results". *Monthly Notices of the Royal Astronomical Society*, **506**, 5046–5074.

[1] https://www.iaumeteordatacenter.org

[2] https://www.ceres.ta3.sk/iaumdcdb/

New meteor shower in Octans

Denis Vida[1], **Damir Šegon**[2] **and Paul Roggemans**[3]

[1] **Department of Earth Sciences, University of Western Ontario, London, Ontario, N6A 5B7, Canada**
denis.vida@gmail.com

[2] **Astronomical Society Istra Pula, Park Monte Zaro 2, 52100 Pula, Croatia**

[3] **Pijnboomstraat 25, 2800 Mechelen, Belgium**
paul.roggemans@gmail.com

A new meteor shower on a Halley-type comet orbit (T_J = 0.93) has been detected during May 22–24, 2025 by the Global Meteor Network. Meteors belonging to the new shower were observed between 61° < $\lambda_\odot$ < 63.5° from a radiant at R.A. = 349° and Decl.= –80° in the constellation of Octans, with a geocentric velocity of 40.6 km/s. The new meteor shower has been listed in the Working List of Meteor Showers under the temporary name-designation: M2025-K1.

1 Introduction

The GMN radiant map[3] for 23–24 May 2025 shows a concentration of radiants in the constellation of Octans (*Figure 1*). Nineteen meteors were observed by the Global Meteor Network low-light video cameras during 2025 May 22–24. The shower was independently observed by cameras in three countries in the southern hemisphere (Australia, New Zealand, and South Africa).

The shower had a median geocentric radiant with coordinates R.A. = 349.06°, Decl. = –79.83°, within a circle with a standard deviation of ± 1.05 deg (equinox J2000.0).

The radiant drift in R.A. is 4.7° on the sky per degree of solar longitude and 0.9° in Decl., both referenced to solar longitude 62.3°. The median geocentric, Sun-centered ecliptic longitude (λ–$\lambda_\odot$) being 229.94°, and geocentric ecliptic latitude –62.86°. The geocentric velocity was 40.6 ± 0.3 km/s.

The new meteor shower has been reported to the IAU-MDC and added in the Working List of Meteor Showers under the temporary name-designation: M2025-K1 (Vida and Šegon, 2025).

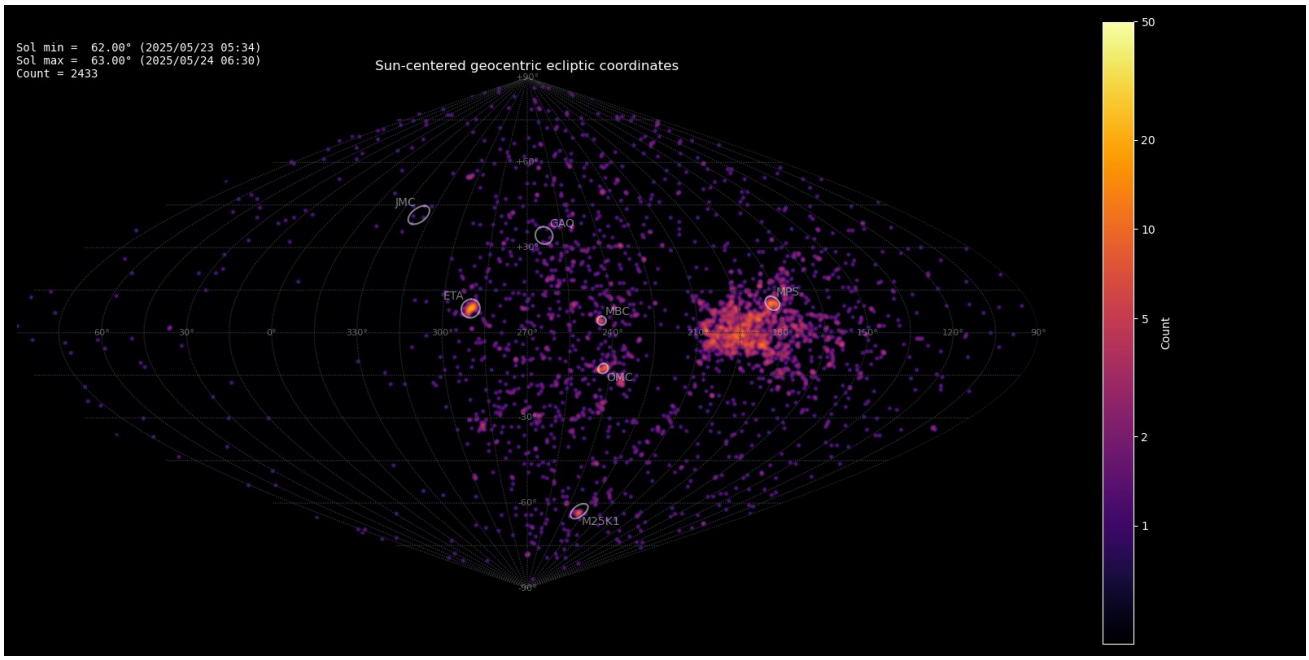

Figure 1 – Heat map with 2433 radiants obtained by the Global Meteor network on 23–24 May 2025. A compact concentration is visible in Sun-centered geocentric ecliptic coordinates which was identified as a new meteor shower with the temporary identification M2025-K1.

[3] https://globalmeteornetwork.org/data/

2 First identification

The Railey distribution fit pointed at a D_D value of 0.09 as the orbital similarity cutoff (*Figure 2*), which resulted in 150 orbits representing the possibly new meteor shower.

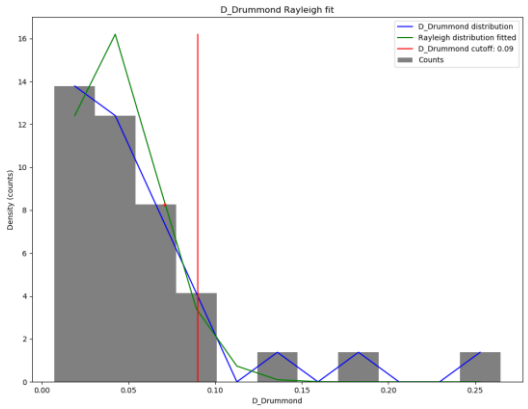

Figure 2 – Rayleigh distribution fit and Drummond D_D criterion cutoff.

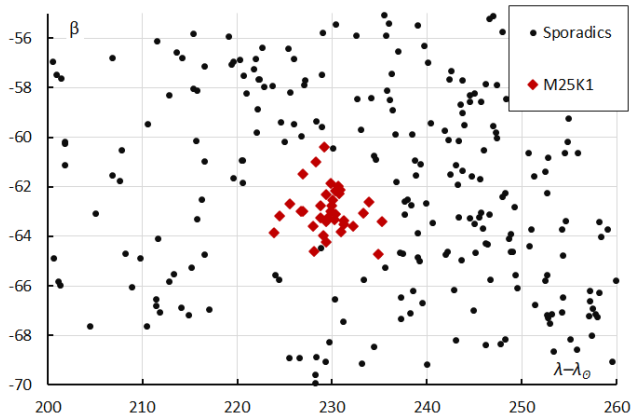

Figure 3 – The radiant in geocentric Sun-centered ecliptical coordinates for the 35 orbits identified as M2025-K1.

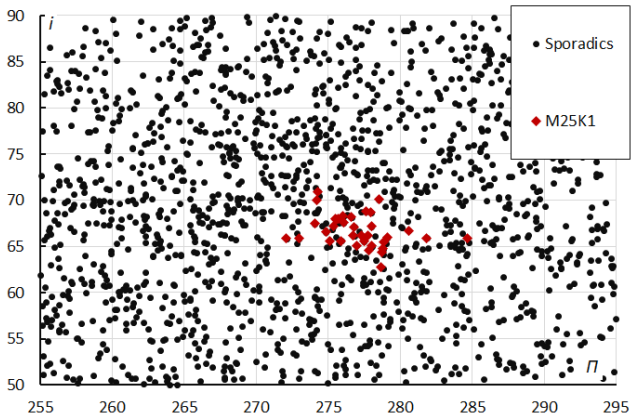

Figure 4 – The diagram of the inclination i against longitude of perihelion Π shows a distinct group of radiants identified as M2025-K1.

The GMN shower association criterion assumes that meteors within 1° in solar longitude, within 3° in radiant, and within 10% in geocentric velocity of a shower reference location are members of that shower. Further details about the shower association are explained in Moorhead et al. (2020). This is a rather strict criterion since meteor showers often have a larger dispersion in radiant position, velocity and activity period. Using these meteor shower selection criteria, 35 orbits have been associated with the new shower in the GMN meteor orbit database (*Figure 3*). Also, the diagram of the inclination i against longitude of perihelion Π shows a distinct group of radiants identified as M2025-K1 (*Figure 4*).

3 Another search method

Another method has been applied to check this new meteor shower discovery. The starting point here can be any visually spotted concentration of radiant points or any other indication for the occurrence of similar orbits. The method has been described before (Roggemans et al., 2019). The main difference with the method applied in *Section 2* is that three different discrimination criteria are combined in order to have only those orbits which fit different criteria. The D-criteria that we use are these of Southworth and Hawkins (1963), Drummond (1981) and Jopek (1993) combined. Instead of using a cutoff value for the D-criteria these values are considered in different classes with different thresholds of similarity. Depending on the dispersion and the type of orbits, the most appropriate threshold of similarity is selected to locate the best fitting mean orbit as the result of an iterative procedure.

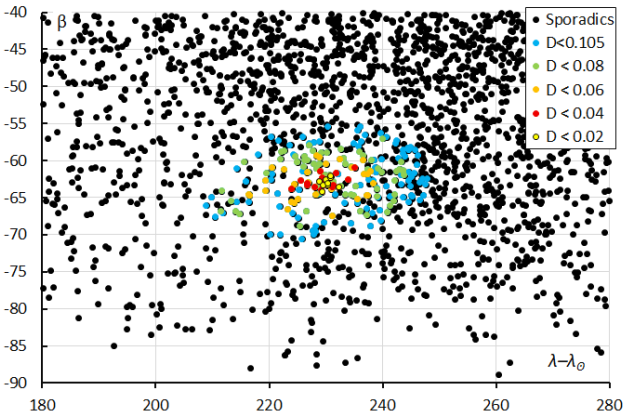

Figure 5 – The radiant in geocentric Sun-centered ecliptical coordinates for different classes of D criterion threshold.

To avoid contamination with sporadics the search interval was limited to $50° < \lambda_\odot < 75°$. The Global Meteor Network had 48411 meteor orbits within this interval. After some iterations the procedure converged on a mean orbit computed following the method of Jopek et al. (2006) with 120 orbits that fit the D-criteria with $D_D < 0.08$. The result is shown in *Figure 5*. Compared to the first method, the selection based on D criteria results in significant more candidates recorded during a longer activity period and much more dispersed radiant distribution.

The dispersion maybe affected by contamination with sporadic particle orbits. The Railey distribution fit as the orbital similarity cutoff with D_D value of 0.09 looks too optimistic. Decreasing the D_D value in steps of 0.01 shows

a concentration comparable to the first method for $D_D = 0.05$. The orbits are compared in *Table 1*.

4 Comparing the results of the two method

Both methods confirm the presence of a new so far unknown minor meteor shower, but there are some differences (see *Table 1*) and it is interesting to visualize these differences. In *Figure 6* the radiant distribution for both methods is shown in a single graph.

Table 1 – Comparing the new meteor shower, derived by two different methods, M2025-K1 the orbital parameters as initially derived, $D_D < 0.08$ and $D_D < 0.05$ were derived from the method described in Section 3.

	M2025-K1	$D_D < 0.08$	$D_D < 0.05$
$\lambda_\odot$ (°)	62.3	62.29	62.1
$\lambda_{\odot b}$ (°)	61.0	51.0	56.8
$\lambda_{\odot e}$ (°)	63.5	73.6	67.3
α_g (°)	349.1	338.4	347.4
δ_g (°)	–79.8	–79.0	–80.2
$\Delta\alpha_g$ (°)	–4.67	–	–
$\Delta\delta_g$ (°)	–0.90	–	–
v_g (km/s)	40.6	40.8	40.6
λ_g (°)	292.38	293.4	291.7
$\lambda_g - \lambda_\odot$ (°)	230.08	229.9	229.4
β_g (°)	–62.83	–62.6	–63.0
a (A.U.)	11.2	10.0	11.6
q (A.U.)	0.927	0.919	0.922
e	0.917	0.908	0.920
i (°)	66.6	67.4	66.6
ω (°)	34.4	34.5	34.8
Ω (°)	242.2	242.7	241.7
Π (°)	276.6	277.1	276.5
T_j	0.93	0.97	0.91
N	19	120	36

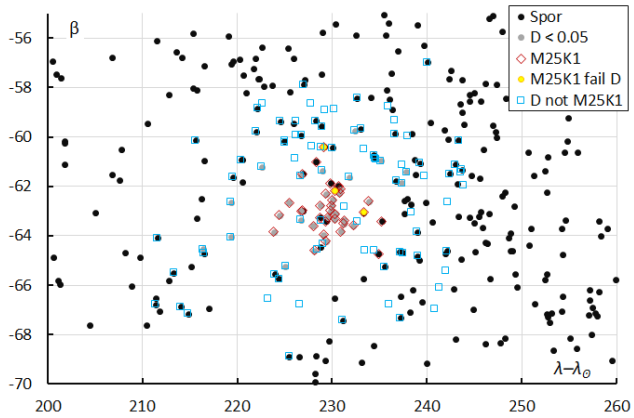

Figure 6 – Comparing the radiant in geocentric Sun-centered ecliptical coordinates obtained by two different methods.

Comparing the radiants associated according to the two methods we see that:

- The 36 grey dots with $D_D < 0.05$ have the best overlap with the red open diamonds that represent the 35 radiants that were identified by the first method. Note that several grey dots were not identified as M2025-K1 by the first method, while several red diamonds did not match $D_D < 0.05$, three of them don't even fulfill $D_D < 0.105$ (yellow circles).
- The 88 blue squares mark radiants that fulfill $D_D < 0.08$ and which were not identified as M2025-K1 in the GMN orbit dataset. The sporadic radiants (black dots) are plotted for the time interval $55° < \lambda_\odot < 65°$. The open blue squares are orbits with $D_D < 0.08$ detected before $\lambda_\odot = 55°$ or after $\lambda_\odot = 65°$.

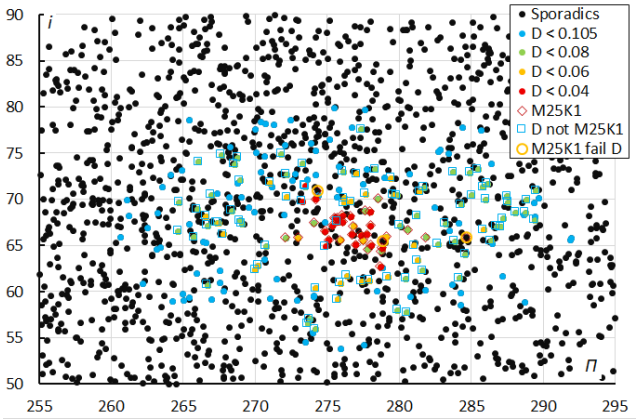

Figure 7 – The diagram of the inclination i against the longitude of perihelion Π for different classes of D criterion threshold and the differences between both meteor shower identification methods.

Figure 7 shows the distribution of the orbits with the inclination i against longitude of perihelion Π for the orbits identified as M2025-K1 by the first method, the result of the second method based on D-criteria and differences between both methods as explained above for *Figure 6*.

5 Orbit and parent body

The Tisserand's parameter T_j identifies the orbit as of a Halley-type comet. A parent-body search returned no candidates with a Southworth and Hawkings D criterion value lower than 0.35. The new shower received the working designation M2025-K1 from the IAU Meteor Data Center.

The mean orbit obtained for the initial 19 orbits on which the discovery was based agrees very well with the mean orbit based on the D-criteria for 36 orbits with $D_D < 0.05$. Even the mean orbit for 120 events with $D_D < 0.08$ compares very well, even though this selection may include some sporadic contamination. We used a new tool to visualize meteor orbits, developed by Pető Zsolt to plot both mean orbits (*Figure 8*). With an aphelion beyond the orbit of planet Uranus, both plots are almost identical.

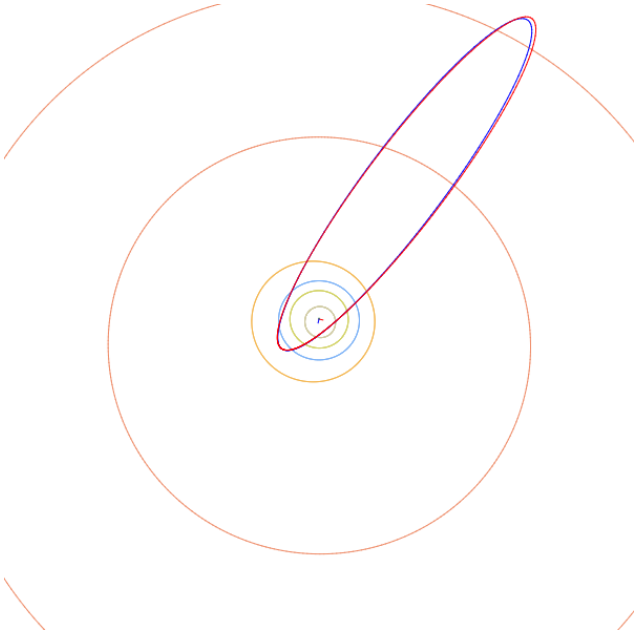

Figure 8 – Comparing the mean orbit based on the shower identification according to two methos, blue is for M2025-K1 and red for $D_D < 0.05$ in *Table 1.* (Plotted with the Orbit visualization app provided by Pető Zsolt).

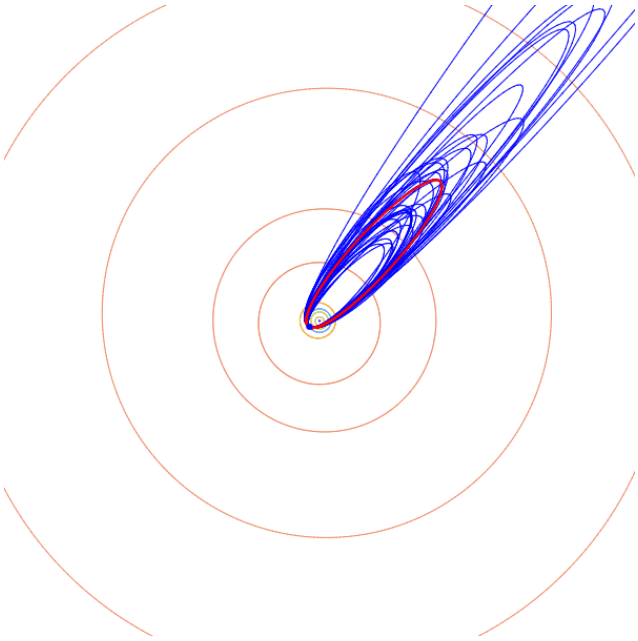

Figure 9 – All 36 orbits based on $D_D < 0.05$ (blue) and their mean orbit (red). (Plotted with the Orbit visualization app provided by Pető Zsolt).

Using a meteor trajectory in our atmosphere to obtain its orbit in the Solar System is very sensitive to measurement uncertainties of both the direction of the trajectory (radiant) and the velocity. The slightest uncertainty on the velocity has a huge effect on the eccentricity and aphelion. For this reason, GMN applies high quality validations. Not all combinations in meteor triangulations yield reliable orbits, therefore quality selection is very important.

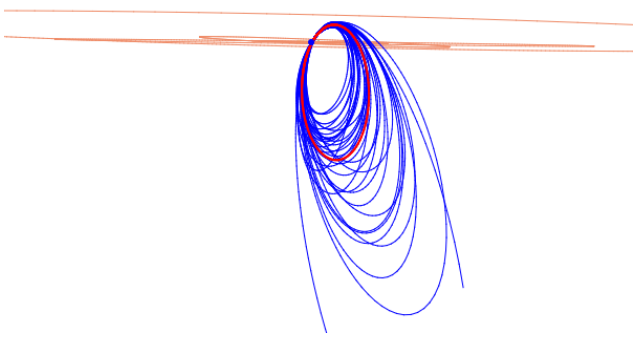

Figure 10 – All 36 orbits based on $D_D < 0.05$ (blue) and their mean orbit (red) as seen in the ecliptic plane. (Plotted with the Orbit visualization app provided by Pető Zsolt).

We used the tool to visualize meteor orbits, developed by Pető Zsolt to plot all 36 orbits (blue) with $D_D < 0.05$ in *Figure 12* seen perpendicular on the ecliptic and seen in the ecliptic plane in *Figure 13*. The mean orbit is computed using the method of Jopek et al. (2006), the dispersion on the individual orbits (blue) can be visualized this way.

6 Activity in past years

A search in older GMN orbit data revealed five orbits that fit the $D_D < 0.08$ criterion during the interval $61.1° < \lambda_\odot < 64.2°$. 28 similar orbits were recorded in 2023, fourteen of these within the interval $60° < \lambda_\odot < 64°$. In 2024 GMN had 36 orbits that fit the D criteria, only six of these in the time interval $60° < \lambda_\odot < 64°$.

7 Conclusion

The discovery of a new meteor shower with a radiant in the constellation of Octans based on nineteen meteors during 2025 May 22–24 has been confirmed. Meanwhile 35 orbits were identified as M2025-K1 in the GMN meteor orbit dataset. The new shower has also been confirmed by an independent meteor shower search method based on D-criteria. The resulting mean orbits for both search methods are in good agreement. The activity period is longer than initially assumed and orbits of this meteor shower have been recorded in past years.

Acknowledgment

This report is based on the data of the Global Meteor Network (Vida et al., 2020a; 2020b; 2021) which is released under the CC BY 4.0 license[4]. We thank all 825 participants in the Global Meteor Network project for their contribution and perseverance. A list with the names of the volunteers who contribute to GMN has been published in the 2024 annual report (Roggemans et al., 2025).

References

Drummond J. D. (1981). “A test of comet and meteor shower associations”. *Icarus*, **45**, 545–553.

[4] https://creativecommons.org/licenses/by/4.0/

Jopek T. J. (1993). “Remarks on the meteor orbital similarity D-criterion”. *Icarus*, **106**, 603–607.

Jopek T. J., Rudawska R. and Pretka-Ziomek H. (2006). “Calculation of the mean orbit of a meteoroid stream”. *Monthly Notices of the Royal Astronomical Society*, **371**, 1367–1372.

Moorhead A. V., Clements T. D., Vida D. (2020). “Realistic gravitational focusing of meteoroid streams”. *Monthly Notices of the Royal Astronomical Society*, **494**, 2982–2994.

Roggemans P., Johannink C. and Campbell-Burns P. (2019a). “October Ursae Majorids (OCU#333)”. *eMetN Meteor Journal*, **4**, 55–64.

Roggemans P., Campbell-Burns P., Kalina M., McIntyre M., Scott J. M., Šegon D., Vida D. (2025). “Global Meteor Network report 2024”. *eMetN Meteor Journal*, **10**, 67–101.

Southworth R. B. and Hawkins G. S. (1963). “Statistics of meteor streams”. *Smithsonian Contributions to Astrophysics*, **7**, 261–285.

Vida D., Gural P., Brown P., Campbell-Brown M., Wiegert P. (2020a). “Estimating trajectories of meteors: an observational Monte Carlo approach - I. Theory”. *Monthly Notices of the Royal Astronomical Society*, **491**, 2688–2705.

Vida D., Gural P., Brown P., Campbell-Brown M., Wiegert P. (2020b). “Estimating trajectories of meteors: an observational Monte Carlo approach - II. Results”. *Monthly Notices of the Royal Astronomical Society*, **491**, 3996–4011.

Vida D., Šegon D., Gural P. S., Brown P. G., McIntyre M. J. M., Dijkema T. J., Pavletić L., Kukić P., Mazur M. J., Eschman P., Roggemans P., Merlak A., Zubrović D. (2021). “The Global Meteor Network – Methodology and first results”. *Monthly Notices of the Royal Astronomical Society*, **506**, 5046–5074.

Vida D., Šegon D. (2025). “New meteor shower in Octans”. D.W.E. Green, editor, CBET 5559.

Quadrantids in 2025: a weak maximum?

Koen Miskotte

Dutch Meteor Society
k.miskotte@upcmail.nl

The Quadrantids showed a relatively weak maximum in 2025 with a *ZHR* of 60 to 70. The maximum was missed visually because it took place above the Pacific Ocean. According to radio and GMN observations the maximum occurred at $\lambda_\odot = 283.0°$. This is 3.4 hours earlier than what was normally expected at $\lambda_\odot = 293.15°$ (Rendtel, 2025). A large subpeak with a *ZHR* of 50 observed at $\lambda_\odot = 283.3°$ (January 3, 2025 ~20^h30^m UT) matches nicely with the subpeak in the Global Meteor Network data.

1 Introduction

The new year always starts with an interesting meteor shower: the Quadrantids. This shower with medium-fast meteors is active between December 25 and January 15. It usually shows a short maximum around $\lambda_\odot = 283.15°$ (Rendtel, 2025). Sometimes the maximum is a bit earlier or later. The observed maximum ZHRs varied quite a bit, years with weak activity have a maximum ZHR of 60, but in good years the ZHR can rise to above 150. For example, in 1995 a ZHR of 110 was found based on DMS observations (Jenniskens et al., 1997). That year the maximum night also resulted in dozens of high-precision orbits of the Quadrantids. Among other things, with this, Peter Jenniskens succeeded in discovering the suspected parent body asteroid 2003 EH1 in a minor planet database of NASA J.P.L. This celestial body may also be the same as comet C/1490 Y1 that has been observed from China. So, it is not an asteroid but probably an extinct comet (Jenniskens, 2006).

The meteor shower also surprised meteor observers in 2009. On the freezing cold night of 2–3 January, European observers observed activity that was well above what was expected. At the end of the night, the ZHR was just around 100, while the maximum occurred around 10^h UT ($\lambda_\odot = 283.039°$) with a ZHR of over 140 (Johannink and Miskotte, 2009). This was 16 years ago, so in 2025 we were looking at approximately the same solar longitude.

In 2025, the conditions for observing the Quadrantids were favorable with a narrow crescent moon that set after 21 hours local time. The maximum was expected on 3 January around 15^h UT ($\lambda_\odot = 283.15°$) (Rendtel, 2025). This means for Europe slowly increasing Quadrantid frequencies during the night. America could then expect the highest activity, but the maximum would not be visible there either if it tooks place at $\lambda_\odot = 283.15°$, this would be situated above the Pacific. The night of 3–4 January then gives rapidly decreasing ZHRs above Europe. And this also with a very low radiant position also playing a role during a large part of the night at the more northern locations. All this is not really favorable for an analysis of the peak activity, but we can perhaps say something about the maximum based on the increasing activity in combination with worldwide radio and GMN observations.

2 Data and method

First, the data was checked on the IMO website. There, 31 observers observed 936 Quadrantids in 55 sessions. That is not much when you consider that the meteor shower can reach a high ZHR. The distribution of the observers was traditional again: many observers active in Europe, a few in America and 9 from Asia. It is important to mention that 8 of the 9 Asian observers observed in Israel. As always, the data had to meet the following requirements:

- A reliable C_p must be known from the observer
- Minimum limiting magnitude 5.9
- A minimum radiant height of 25 degrees
- Maximum cloud cover correction $k = 1.10$

In addition to the night of 2–3 January, many observations were also made in the evening of 3 January in Europe. The radiant height was usually below the minimum 25-degree height limit. That is why the minimum radiant height for the maximum was set lower, to 10 degrees. The zenith attraction of the radiant has also been taken into account. Since Quadrantids have a geocentric velocity of 41 km/sec, this has only been done for radiant positions below 25 degrees, the differences above 25 degrees are rather small (Rendtel, 2022).

3 Population index *r*

From the observations, the population index *r* could be calculated according to Steyaert (1981). The results of these computations are shown in *Table 1* and *Figure 1*. This gives a result that is recognizable for the Quadrantids. A somewhat higher population index *r* before the maximum and a somewhat lower population index *r* after the maximum. The low *r* value of January 3, 2025 around 0^h30^m UT is mainly caused by the lack of weak Quadrantids compared to the bright meteors.

Table 1 – Population index *r*[–1;5] Quadrantids 2025 based on 500 Quadrantids, all for the date 03 January 2025.

Time UT	$\lambda_\odot$ (°)	*r*[–1;5]	QUA
0.50	282.529	1.55 ± 0.45	30
1.50	282.572	2.44 ± 0.37	42
2.50	282.614	2.54 ± 0.31	55
3.50	282.657	2.89 ± 0.4	37
5.45	282.740	2.67 ± 0.2	114
9.08	282.894	2.70 ± 0.43	33
9.87	282.927	2.50 ± 0.43	33
11.03	282.977	2.54 ± 0.3	59
17.00	283.230	2.44 ± 0.43	34
17.50	283.252	2.29 ± 0.51	25
18.50	283.294	2.43 ± 0.39	38

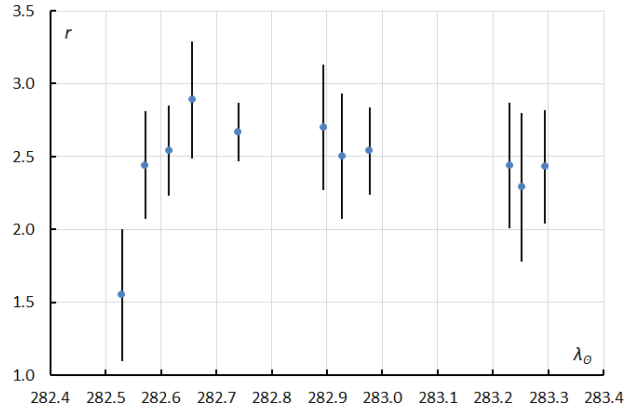

Figure 1 – Population index *r* [–1;5] Quadrantids 2025.

4 Zenithal Hourly Rate

After calculating the population index *r*, the minimum radiant height was first calculated at 25 degrees. This was then done again with a minimum radiant height of 10 degrees. The formula used to calculate the *ZHR* is:

$$ZHR = \frac{n \cdot r^{6.5-lm}}{(\sin h)^{\gamma} \cdot C_p \cdot T_{eff}}$$

The gamma was set to 1 instead of 1.4 (Jenniskens, 1994). This resulted in *Table 2* and *Figures 2 and 3*.

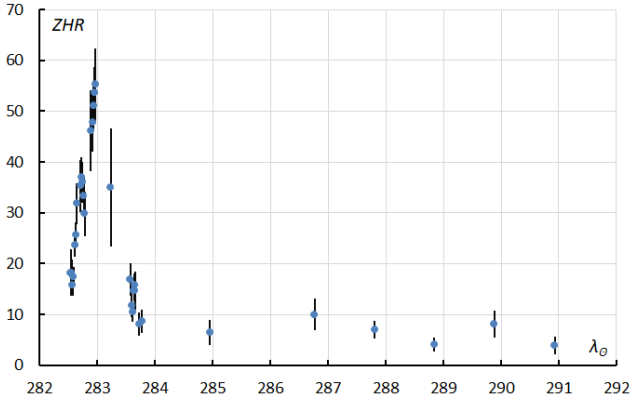

Figure 2 – *ZHR* of the Quadrantids between January 3 and 11, 2025. *ZHR* were calculated with radiant heights above 25°.

Table 2 – *ZHR* for the Quadrantids 2025 with radiant elevation above 10°. T_m = mean time, *P* is number of periods.

Day	T_m UT	$\lambda_\odot$	*P*	QUA	*ZHR*
2	20.07	282.341	2	4	8.7 ± 4.4
2	20.78	282.371	2	4	8.3 ± 4.2
2	23.8	282.500	4	9	16.5 ± 5.5
3	0.10	282.513	9	27	19.1 ± 3.7
3	0.55	282.531	11	36	19.6 ± 3.3
3	1.11	282.555	17	56	18.4 ± 2.5
3	1.52	282.573	20	59	15.8 ± 2.1
3	1.97	282.592	22	87	17.5 ± 1.9
3	2.51	282.612	20	113	23.6 ± 2.2
3	2.94	282.633	16	98	25.6 ± 2.6
3	3.22	282.645	10	63	31.8 ± 4.0
3	4.75	282.710	5	47	35.3 ± 5.1
3	5.17	282.728	8	91	37.0 ± 3.9
3	5.54	282.744	7	83	36.0 ± 4.0
3	6.05	282.765	7	88	33.3 ± 3.5
3	6.41	282.781	5	47	29.8 ± 4.3
3	8.77	282.881	2	44	51.6 ± 7.8
3	9.63	282.917	3	67	49.9 ± 6.1
3	10.17	282.940	4	108	51.0 ± 4.9
3	10.47	282.953	4	116	53.6 ± 5.0
3	10.77	282.966	2	61	55.2 ± 7.1
3	17.18	283.238	10	64	30.5 ± 3.8
3	17.45	283.249	12	73	31.8 ± 3.7
3	18.08	283.276	9	35	29.8 ± 5.0
3	18.42	283.291	10	34	26.5 ± 4.5
3	18.91	283.311	9	29	24.1 ± 4.5
3	19.48	283.336	9	34	28.8 ± 4.9
3	19.92	283.354	8	36	34.8 ± 5.8
3	20.53	283.380	6	42	50.9 ± 7.9
3	23.50	283.506	5	7	13.8 ± 5.2
4	0.00	283.528	5	8	11.3 ± 4.0
4	0.58	283.533	7	22	19.4 ± 4.1
4	1.03	283.572	9	27	16.9 ± 3.3
4	1.58	283.595	11	27	11.8 ± 2.3
4	1.97	283.611	13	32	10.4 ± 1.8
4	2.56	283.636	15	54	14.6 ± 2.0
4	2.80	283.646	11	44	15.7 ± 2.4
4	3.03	283.657	4	15	14.7 ± 3.8
4	4.74	283.729	3	13	8.1 ± 2.2
4	5.83	283.775	2	15	8.7 ± 2.2
5	9.51	284.951	3	7	6.5 ± 2.5
7	4.26	286.766	2	10	10.0 ± 3.2
8	4.92	287.813	3	16	7.0 ± 1.8
9	5.17	288.843	3	10	4.1 ± 1.3
10	5.60	289.880	2	9	8.1 ± 2.7
11	6.44	290.934	2	5	3.9 ± 1.7

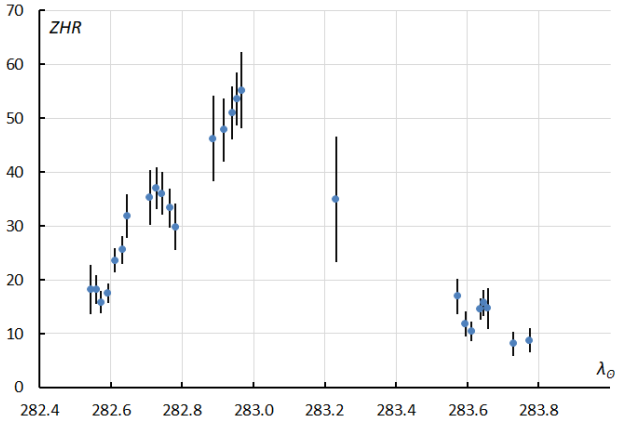

Figure 3 – *ZHR* of the Quadrantids between 3 January 2025, 0^h UT and 4 January 2025, 6^h UT. *ZHR*s were calculated with radiant heights higher than 25°.

Next, calculations were repeated with radiant heights from 10 degrees, whereby a correction was made for zenith attraction between 10 and 25 degrees of height. This resulted in *Figure 4*.

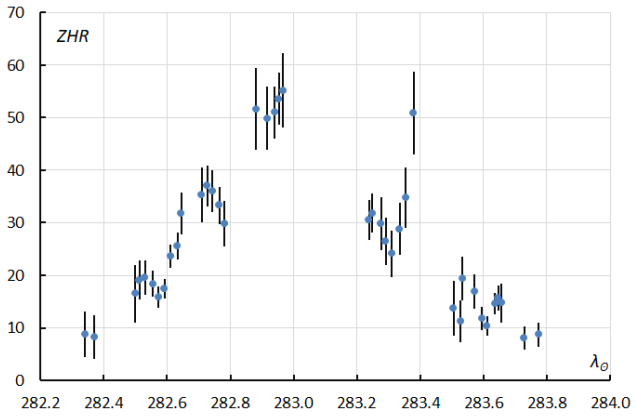

Figure 4 – *ZHR* of the Quadrantids between 3 January 2025, 0^h UT and 4 January 2025, 6^h UT. *ZHR* with radiant heights higher than 10 degrees.

It is noticeable in *Figure 4* that the activity above Europe starts with low *ZHR*s of 16 and then to rise to a maximum *ZHR* of 37 during the night of Januari 2–3. Then the *ZHR* decreased to around 30 at the end of the night. When it got dark in North America, Terrence Ross and Pierre Martin, among others, saw a beautiful Quadrantid show. The *ZHR* rose from 50 to 60 during their observation period.

When it got dark again in Europe, the Quadrantid maximum was over and the *ZHR* was already dropping to around 30 and further decreasing. But then the *ZHR* rose again quite quickly to a *ZHR* of 50 around $\lambda_\odot = 283.3$ (January 3, 2025 ~20^h30^m UT). A subpeak it seems, unfortunately Jürgen and Ina Rendtel, who observed this peak at the same location, had to stop due to cloud cover. Too bad that at that time there were no more observers active who could confirm this extra peak. All this with low radiant heights also causes somewhat larger deviations. When the Israeli observers started a few hours later (the Quadrantid radiant is not circumpolar in Israel and does not appear there until around 23^h UT), the *ZHR* had already dropped back to *ZHR* values between 10 and 20.

5 Visual observations compared to global radio and GMN observations

In order to see if the visual subpeak is also visible in the radio observations, Hiroshi Ogawa & Hirofumi Sugimoto were asked for observational data from the radio observers. This data was put in the visual graph to see if the behavior is the same. Note that this data cannot be seen as 1 on 1, after all, these are two very different observation techniques. The result can be seen in *Figure 5*. Overall, the trend is the same. There is also a subpeak in the radio observations, but this occurred 3 hours earlier than the visually observed subpeak. So, no confirmation of the visual peak can be concluded from the radio observations.

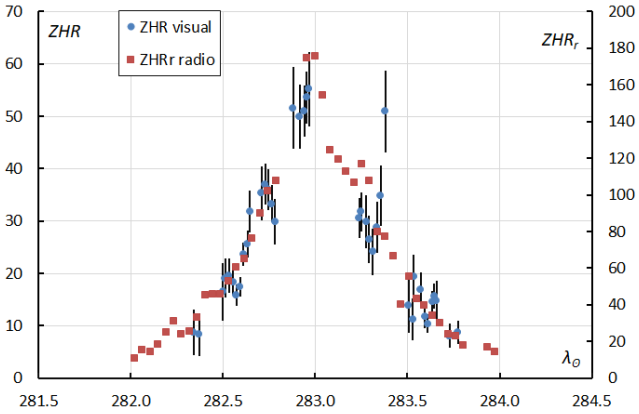

Figure 5 – The visual *ZHR* curve compared to the radio ZHR_r curve. The radio ZHR_r curve is scaled to the visual *ZHR* curve to see if the progression matches.

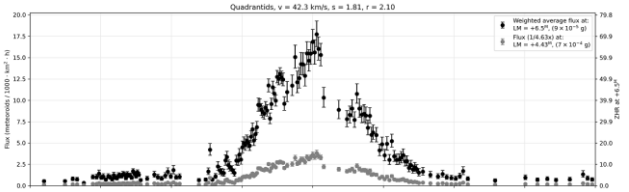

Figure 6 – The GMN flux and ZHR profile of the Quadrantids in 2025 (Vida et al., 2021; 2022).

Next, the ZHR profile of the Quadrantids was checked up in the GMN database[5] to compare with the radio and visual reasults. There is also a subpeak visible and appears at almost the same time as the visual subpeak. A compliment to the visual observers who observed this so beautifully, despite the low radiant position.

Both GMN and the radio ZHR_r profile show the maximum exactly at $\lambda_\odot = 283.0°$. This is 3.4 hours earlier than the expected maximum at $\lambda_\odot = 283.15°$. Pierre Martin's observation at $\lambda_\odot = 282.97°$ (January 3, 2025 at 10^h55^m UT) is the closest to the maximum found by GMN and radio observers at $\lambda_\odot = 283.0°$ (January 3, 2025 at 11^h36^m UT). His highest *ZHR* value was indeed in that last hour with a *ZHR* of 55 ± 7. GMN finds a *ZHR* of just below 60 at that

[5] https://globalmeteornetwork.org/flux/plots/

same time and GMN's maximum *ZHR* value with a *ZHR* of 70 some 40 minutes later matches nicely.

6 Conclusion

The Quadrantids showed a relatively weak maximum in 2025 with a *ZHR* of 60 to 70. The maximum was missed visually because it took place above the Pacific Ocean. According to radio and GMN observations the maximum occurred at $\lambda_{\odot} = 283.0°$. This is 3.4 hours earlier than what was normally expected at $\lambda_{\odot} = 293.15°$ (Rendtel, 2025). A large subpeak with a *ZHR* of 50 observed at $\lambda_{\odot} = 283.3°$ (January 3, 2025 ~$20^{h}30^{m}$ UT) matches nicely with the subpeak in the Global Meteor Network data.

Acknowledgments

A word of thanks to all the visual observers who observed the Quadrantids. These are: *Mark Adams, Orlando Benítez Sánchez, Felix Bettonvil, Ido Braun, Steve Brown, Tal Dagan, Kai Gaarder, Christoph Gerber, Noa Ginzberg, Javor Kac, Omri Katz, Ralf Koschack, Anna Levin, Andreas Livbom, Pierre Martin, Koen Miskotte, Mohammad Nilforoushan, Ella Ratz, Ina Rendtel, Jürgen Rendtel, Fillip Romanov, Terrence Ross, Ulrich Sperberg, Tamara Tschenak, David Teissier, Snežana Todorović, Michel Vandeputte, Ariel Westfried, Roland Winkler, Frank Wächter and Sabine Wächter*.

Furthermore, a word of thanks to *Carl Johannink* and *Michel Vandeputte* for reviewing this article. Also, a thank you for *Paul Roggemans* for checking my English. Thanks also to *Hirofumi Sugimoto* and *Hiroshi Ogawa* for providing the radio observations. Finally, a word of thanks to the *Global Meteor Network volunteers and the network administrators*[6].

References

Jenniskens P. (1994). "Meteor stream activity I. The annual streams". *Astronomy and Astrophysics*, **287**, 990–1013.

Jenniskens P., Betlem H., de Lignie M., Langbroek M., Van Vliet M. (1997). "Meteor stream activity. V. The Quadrantids, a very young stream". *Astronomy and Astrophysics*, **327**, 1242–1252.

Jenniskens P. (2006). Meteor Showers and their Parent Comets, p. 357–377, Cambridge University Press.

Johannink C., Miskotte K. (2009). "De Quadrantiden in 2009: een leuke verrassing!". *Radiant*, **31**, 43–50.

Rendtel J. (2022). Handbook for meteor observers, IMO.

Rendtel J. (2025). IMO Meteor Shower Calendar, IMO.

Steyaert C. (1981). "Populatie indexbepaling : methode en nauwkeurigheid". *Technische Nota nr. 5*, VVS Werkgroep Meteoren, september 1981.

Vida D., Šegon D., Gural P. S., Brown P. G., McIntyre M. J. M., Dijkema T. J., Pavletić L., Kukić P., Mazur M. J., Eschman P., Roggemans P., Merlak A., Zubrović D. (2021). "The Global Meteor Network – Methodology and first results". *Monthly Notices of the Royal Astronomical Society*, **506**, 5046–5074.

Vida D., Blaauw Erskine R.C., Brown P.G., Kambulow J., Campbell-Brown M. and Mazur M. J. (2022). "Computing optical meteor flux using global meteor network data". *Monthly Notices of the Royal Astronomical Society*, **515**, 2322–2339.

[6] https://globalmeteornetwork.org/

ERI (#191), RER(#738), THC(#535) and NFC (#931) activity in 2023 recorded by Japan's Sonotaco Network

Takashi Sekiguchi

Nippon Meteor Society and SonotaCo network, Japan
ts007@mtj.biglobe.ne.jp

Known meteor showers have complex structures formed by their parent bodies and their subsequent orbital evolution. The structure can be analyzed by plotting various parameters in diagrams. I analyzed a total of 1812 simultaneous meteors observed in the SonotaCo Network between 2007 and 2024, focusing on 2023, the year with the largest numbers of appearances. We were able to elucidate four groups based on the radiant point (ranging in α from 0° to 70° and in δ from 0° to –25° around ERI) and orbital elements based on the simultaneous meteors from July to August 2023. It has been confirmed that there are two major meteor showers: the three Eridanid meteor showers (ERI#191, RER#738 and THC#535) active in August and the August Ceti 95 meteor shower (NFC#931), which was recently removed from the IAU list. The meteor showers that generate the Eridanid meteor shower association were divided into three groups in function of the velocity and the argument of perihelion ω. Each of these groups is known and assumed to be related to a parent body, while the activity periods coincide by chance. Comparison of orbital elements reveals a correlation between inclination i, perihelion distance q, and the argument of perihelion ω. Due to the long duration of activity, the radiant region is about 50 degrees in right ascension and 20 degrees in declination. The August Eridanids show a concentration, whereas the other two seem to be quite diffuse. Neither meteor shower can be described by a single orbital element. In this paper, we present representative orbits and identifications with meteor showers previously reported in the literature. We also discuss candidates for meteoroids and possible parent bodies. Furthermore, the annual activity of simultaneous meteor showers from July to August in 2007 to 2024 reveals two approximately 6-year periodicities, with a possible increase in 2025.

1 Introduction

Using the SonotaCo Network meteor orbit data from 2007 to 2024, I plotted the distribution of the radiants around ERI (ranging in α from 0° to 70° and in δ from 0° to –25°) meteors using MRaDViewer v1.01[7], and the result is shown in *Figure 1*. I noticed that the meteors were fast but widely dispersed.

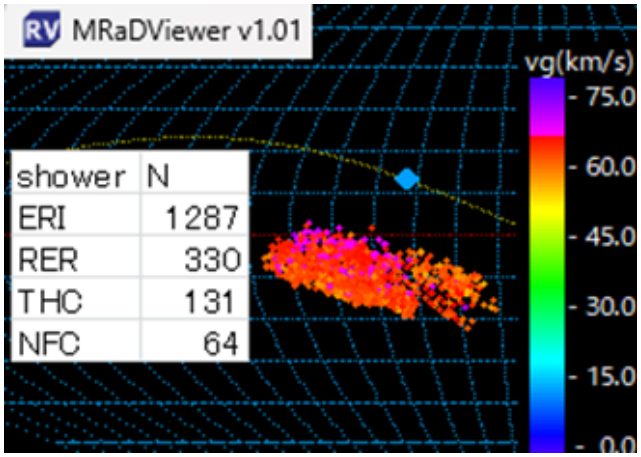

Figure 1 – Graph of the radiant point around ERI.

2 The 2023 activity

I created a graph of their appearance by year. As shown in *Figure 2*, 2023 stood out. I decided to classify only the meteors from 2023. First, the distribution of right ascension and declination of the radiant. *Figure 3* is color-coded by geocentric speed. Most are 58–66 km/sec.

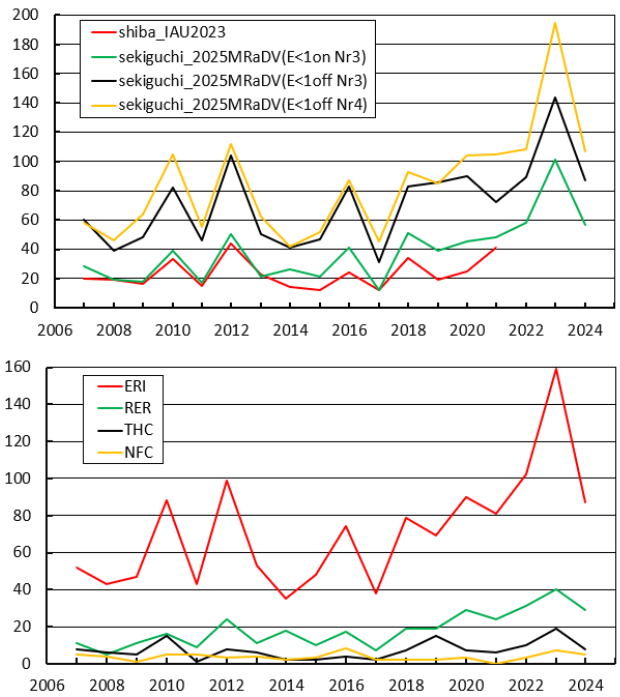

Figure 2 – Graph of annual appearances around ERI.

Next, I tried to classify them using the IAU working list of meteor showers. There seemed to be some misjudgments, so I corrected them using orbital elements, etc. There still

[7] https://sonotaco.jp/forum/viewtopic.php?t=5905

seem to be some misjudgments, but I was able to classify them into four groups as shown in *Figure 4*.

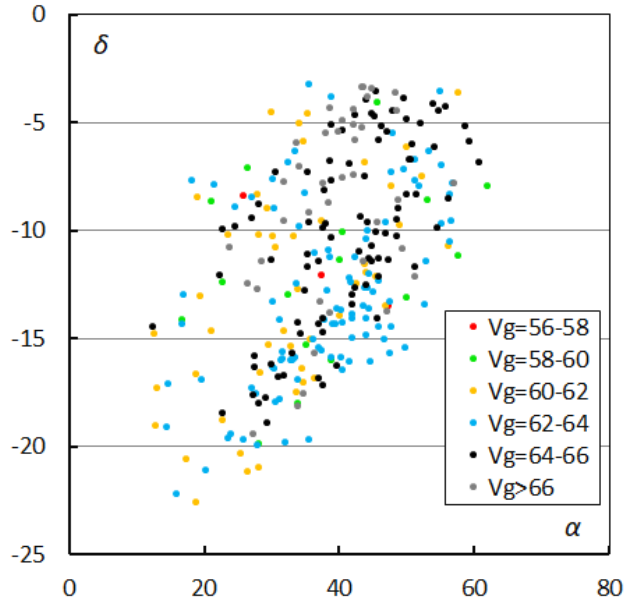

Figure 3 – Plot of the radiant point color-coded by geocentric velocity v_g in 2023.

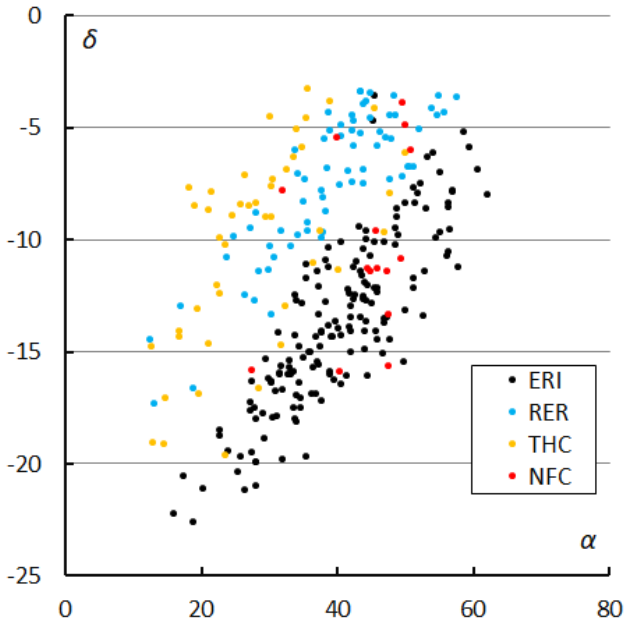

Figure 4 – Plot of the radiant points according to the IAU working list of meteor showers in 2023.

Next, I applied the Southworth and Hawkins criterion, D_{sh} using orbital elements to create a distribution map of right ascension and declination of the radiant for each group. These are *Figures 5 to 8*. In each group, those with small D_{sh} are concentrated in the center, and D_{sh} increases as you move away from the maximum.

Next, I created a graph of the solar longitude and right ascension, shown in *Figure 9*. The movement of the radiant points of the four groups is now clearly visible. Similarly, I created a graph of the solar longitude and declination,

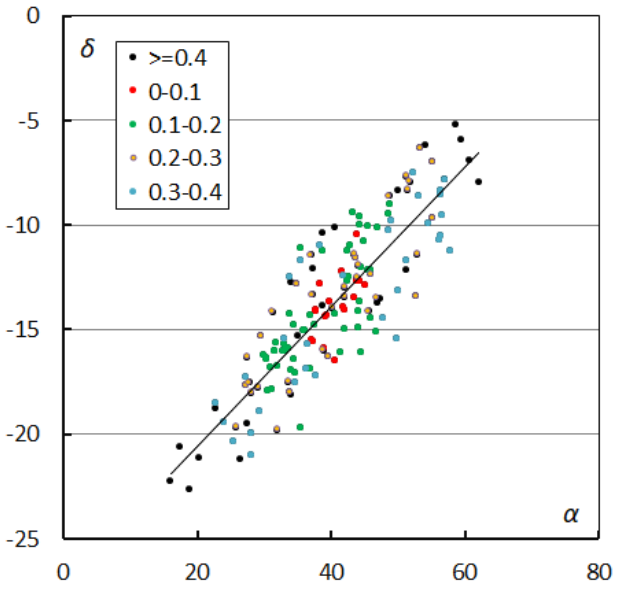

Figure 5 – Plot of the radiant point for ERI by D_{sh}.

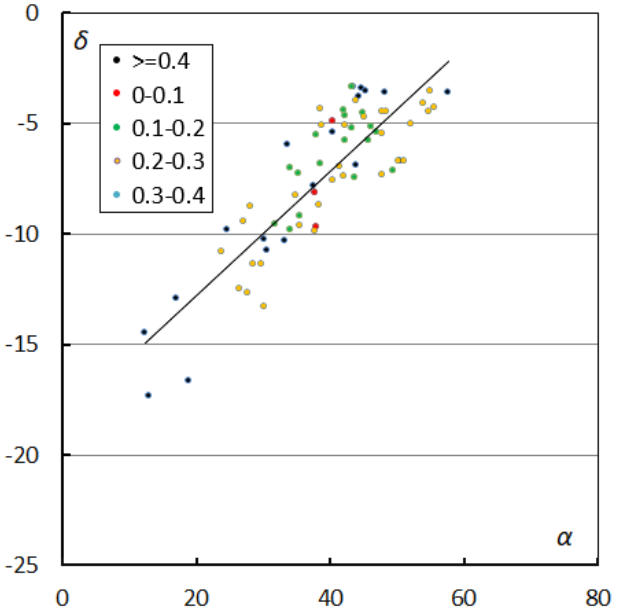

Figure 6 – Plot of the radiant point for RER by D_{sh}.

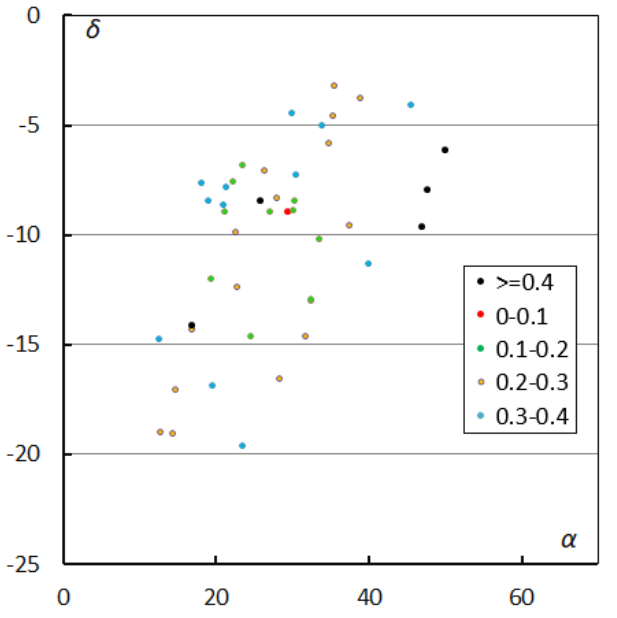

Figure 7 – Plot of the radiant point for THC by D_{sh}.

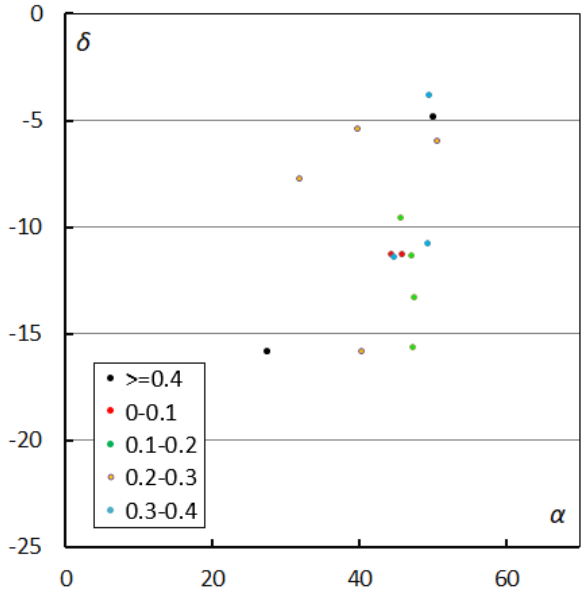

Figure 8 – Plot of the radiant point for NFC by D_{sh}.

shown in *Figure 10*. The movement of the radiant points of the four groups is now clearly visible. Finally, I created a graph of the solar longitude against the geocentric velocity v_g, shown in *Figure 11*. ERI and RER show a slight deceleration, while THC and NFC show a slight acceleration.

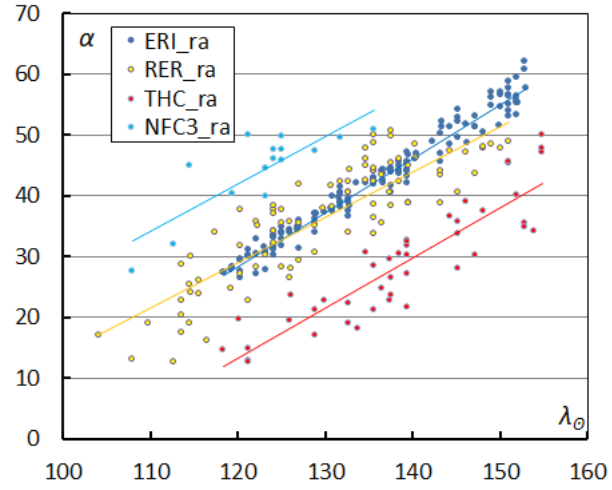

Figure 9 – Graph right ascension in function of solar longitude.

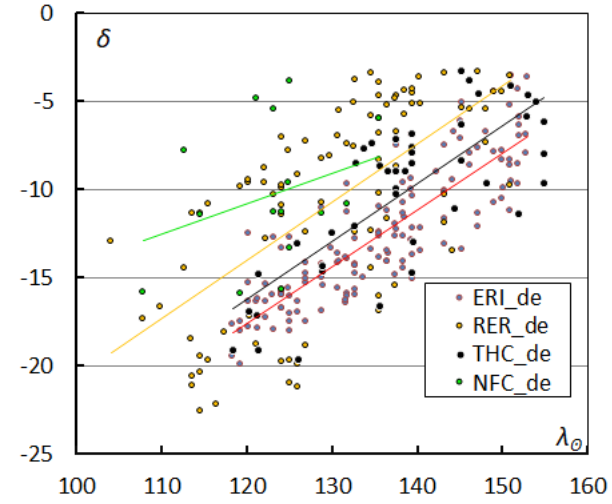

Figure 10 – Graph declination in function of solar longitude.

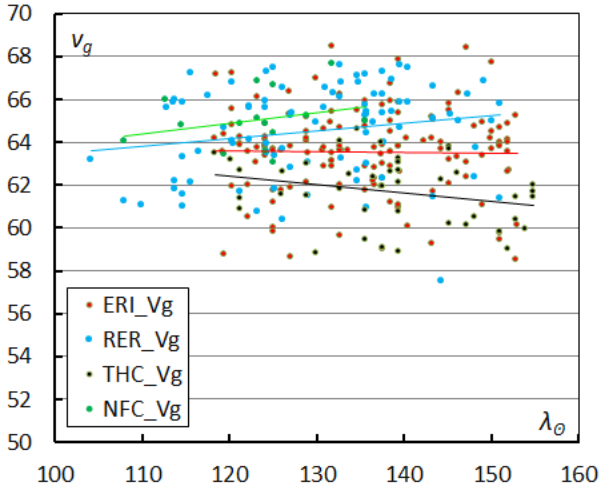

Figure 11 – Graph geocentric velocity in function of solar longitude.

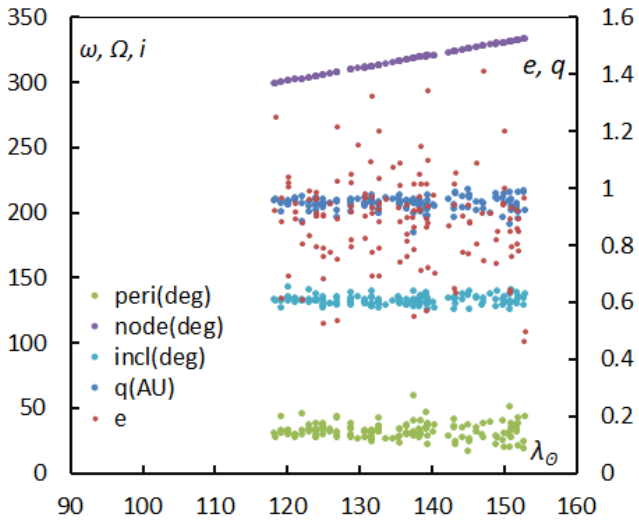

Figure 12 – Graphs of the orbital elements of ERI against solar longitude, argument of perihelion, node and inclination, on the axis at left, eccentricity and perihelion distance at right.

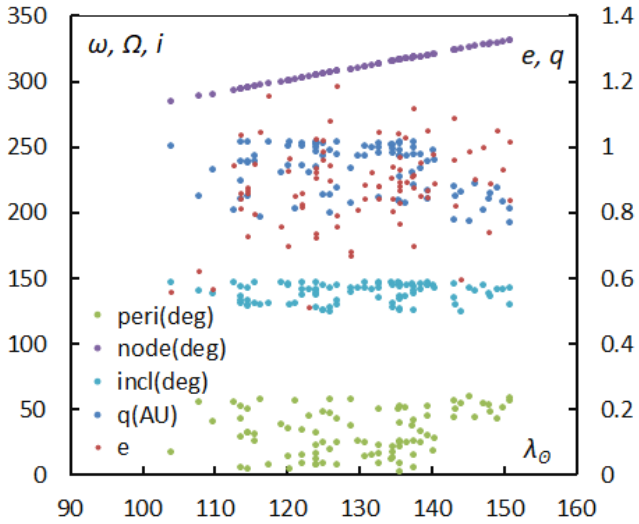

Figure 13 – Graphs of the orbital elements of RER against solar longitude, argument of perihelion, node and inclination, on the axis at left, eccentricity and perihelion distance at right.

I created graphs of the orbital elements against solar longitude. These are shown in *Figures 12 to 15*. ERI, RER, and THC have a slight difference in ω, but only FNC has a

clearly different ω of 250 degrees. The eccentricity e and perihelion distance q are shown enlarged in *Figures 16 to 19*. The concentration and spread are different for each group. *Figure 20* shows the variation in geocentric velocity v_g against declination δ.

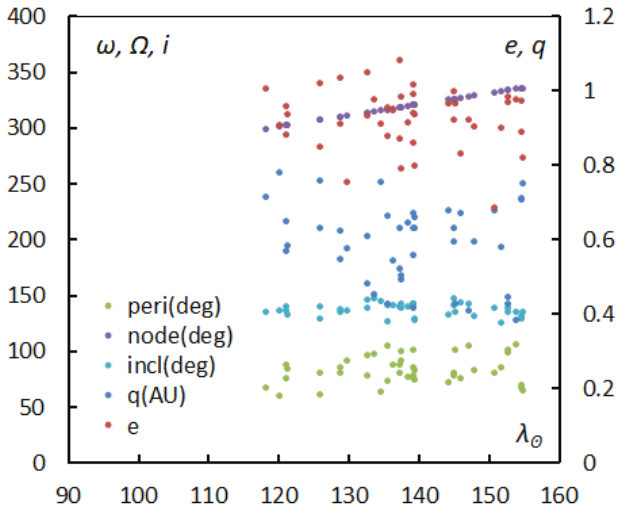

Figure 14 – Graphs of the orbital elements of THC against solar longitude, argument of perihelion, node and inclination, on the axis at left, eccentricity and perihelion distance at right.

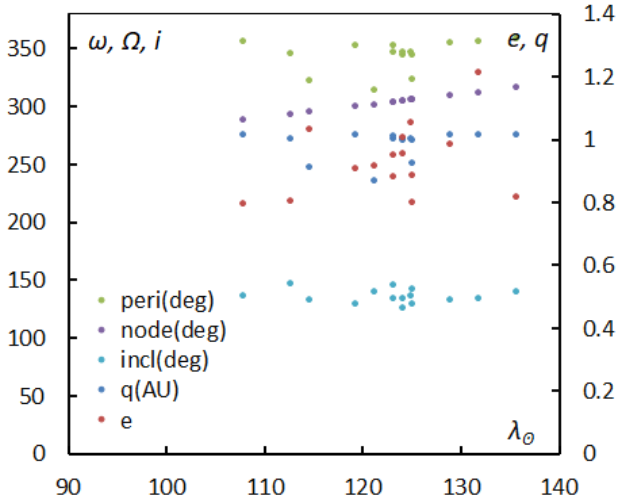

Figure 15 – Graphs of the orbital elements of FNC against solar longitude, argument of perihelion, node and inclination, on the axis at left, eccentricity and perihelion distance at right.

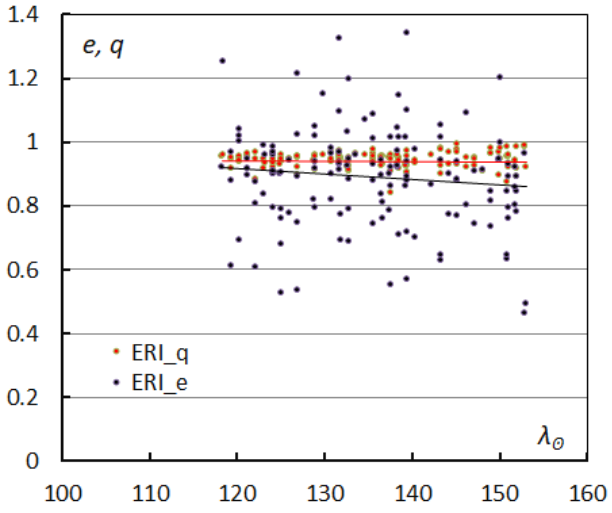

Figure 16 – Graphs of q and e against solar longitude for ERI.

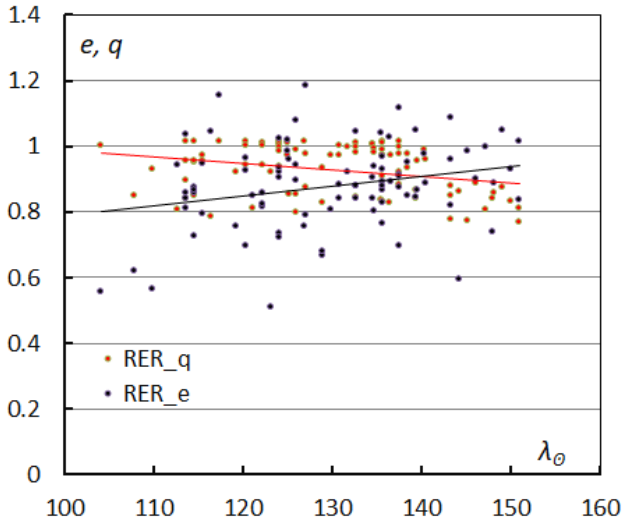

Figure 17 – Graphs of q and e against solar longitude for RER.

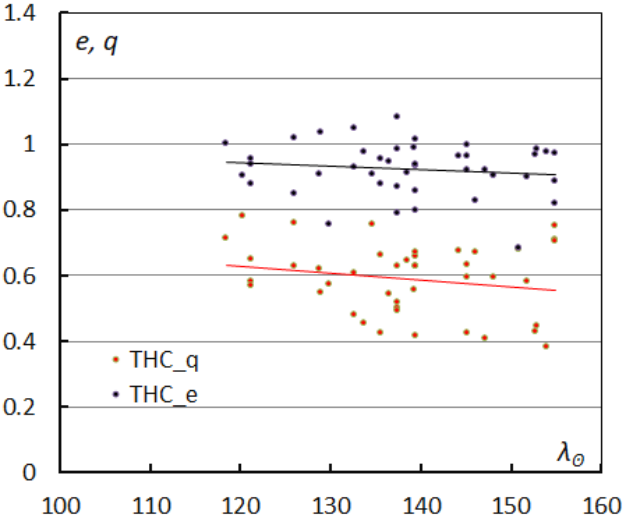

Figure 18 – Graphs of q and e against solar longitude for THC.

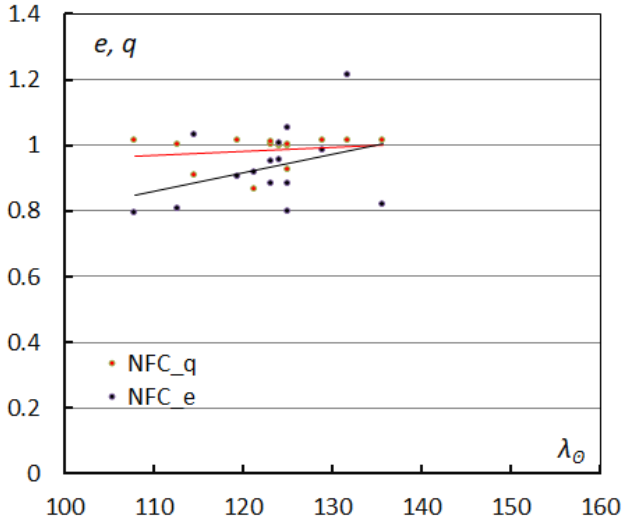

Figure 19 – Graphs of q and e against solar longitude for NFC.

I created a graph of ecliptic longitude λ against ecliptic latitude β. The four groups are neatly scattered, shown in *Figure 21*.

Figure 22 is the diagram of the q–i relationship. Here too, the four groups are well spread out. As expected, ERI is concentrated. THC is quite spread out.

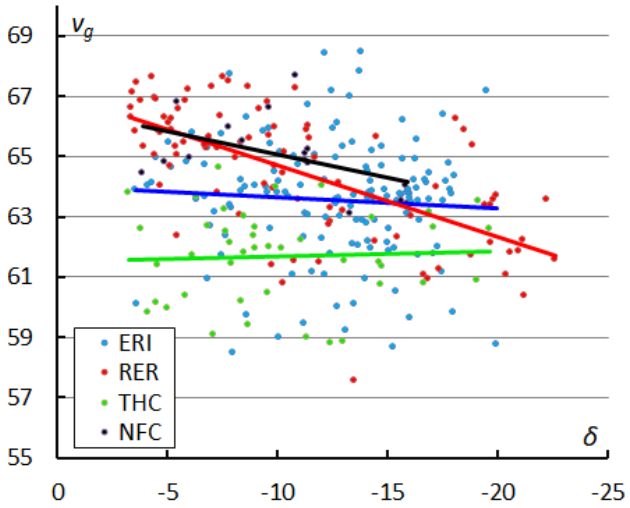

Figure 20 – Graphs of the geocentric velocity against declination.

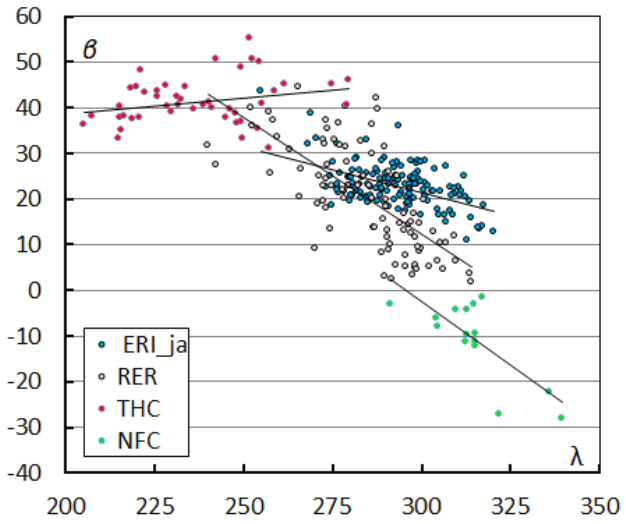

Figure 21 – Graphs of the ecliptic altitude against longitude.

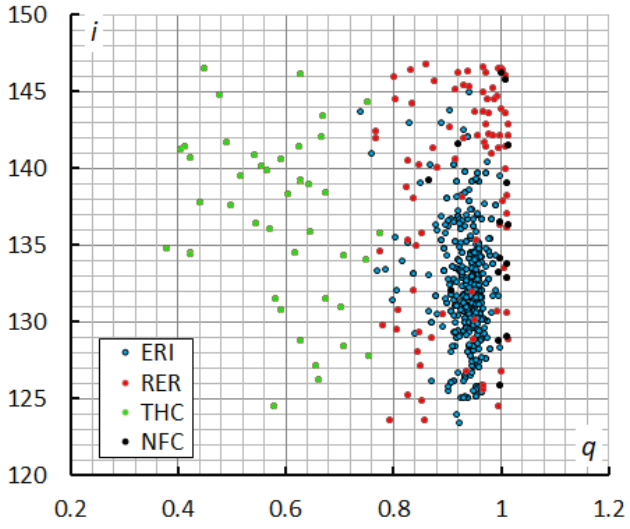

Figure 22 – Diagram of the inclination i against perihelion distance q.

Figure 23 is the diagram of the ω–i distribution. Here too, the four groups are well spread out. As expected, ERI is concentrated. THC is similarly spread out as RER.

Figure 24 is the diagram of the ω–q distribution. Here, ERI and RER cannot be distinguished. THC is in the extension of ERI and RER. FNC is distinguished on the opposite side.

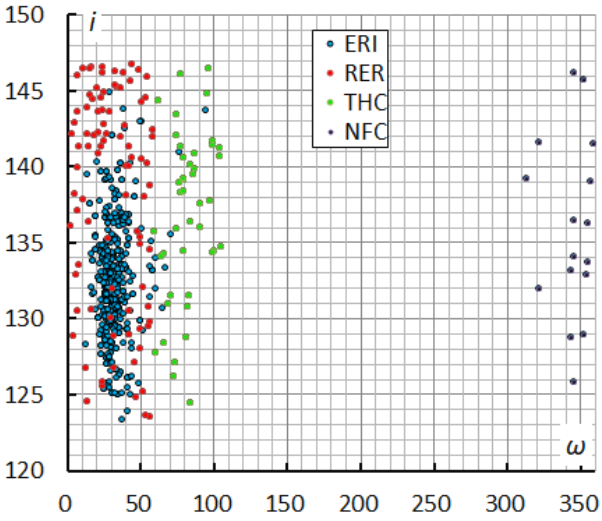

Figure 23 – Diagram of the inclination i against the argument of perihelion ω.

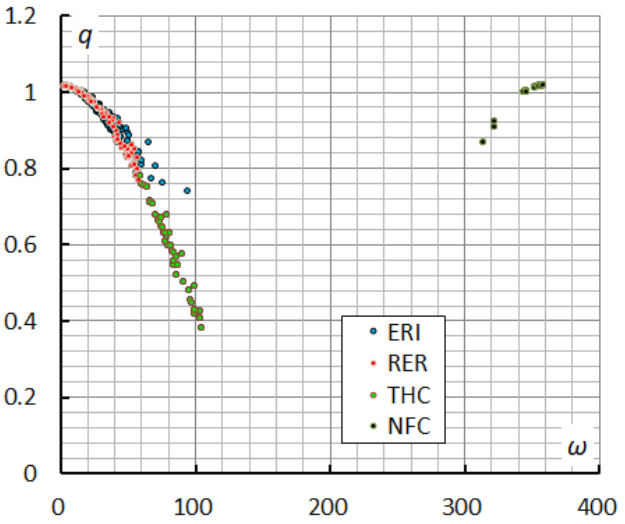

Figure 24 – Diagram of the perihelion distance q against the argument of perihelion ω.

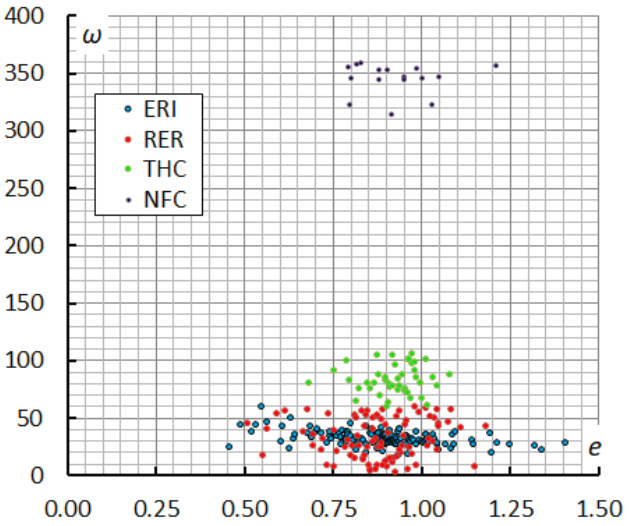

Figure 25 – Diagram of the argument of perihelion ω against eccentricity e.

Figure 25 shows a diagram of the e–ω distribution. Here, ERI is concentrated and RER is spread around it. We can see the velocity spread. THC is on the extension of ERI and RER, and FNC can be distinguished on the upper side.

Finally, *Figure 26* is the diagram of the q–e distribution. Here too, ERI is concentrated, but it is difficult to distinguish between ERI and RER. There are some graphs where it is difficult to distinguish between THC and ERI. FNC is concentrated, but there are some separated cases. I don't know if this is a misjudgment.

3 Orbit

The average orbits of the four groups around ERI (α from 0° to 70° and δ from 0° to –25°) from July to August 2023 were calculated, see *Table 1*.

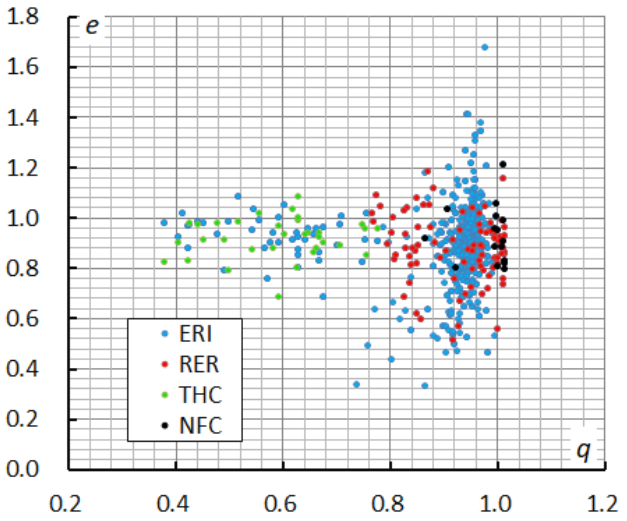

Figure 26 – Diagram of the eccentricity e against the perihelion distance q.

Table 1 – The geocentric radiant and velocity, and other orbital parameters for 2023 data.

Group	$\lambda_\odot$ (°)	α_g (°)	δ_g (°)	v_g (km/s)	a (AU)	q (AU)	e	ω (°)	Ω (°)	i (°)	M_A	dur (sec)	H_B (km)	H_E (km)	λ_{II}	β_{II}
ERI N=142	135.65	42.24	-12.56	63.56	8.56	0.943	0.890	31.56	315.65	132.10	-1.1	0.4	110.7	98.77	293.27	22.85
RER N=89	129.96	42.96	-7.43	64.923	8.46	0.917	0892	33.62	318.43	139.38	-1.1	0.4	109.2	97.51	291.65	21.13
THC N=63	138.55	28.51	-10.15	61.70	7.68	0.589	0.923	82.55	318.55	136.73	-0.8	0.4	108.2	95.07	238.73	42.81
NFC N=13	122.82	44.20	-10.31	65.01	14.47	0.985	0.932	343.9	302.82	135.56	-1.6	0.5	109.4	97.83	314.47	-11.20

Table 2 – Orbit data and orbital elements of the parent body candidates.

Name	a (AU)	e	q (AU)	i (°)	ω (°)	Ω (°)	D_{SH}	T_J	λ_{II}	β_{II}	α_g (°)	δ_g (°)	v_g (km/s)
2023_ERI	8.56	0.890	0.943	132.10	31.56	315.65	0.00	-0.18	293.27	22.85	42.2	-12.6	63.6
IAU_ERI	26.40	0.965	0.951	131.80	29.00	314.80	0.08	-0.61	294.52	21.19	41.8	-13.1	64.4
1852K1	-	1.000	0.905	131.12	37.21	319.27	0.14	-	292.74	27.10	39.6	-13.8	64.5
2023_RER	8.46	0.892	0.917	139.38	29.00	314.80	0.00	-0.26	291.65	21.13	43.0	-7.4	64.9
IAU_ERI	26.40	0.965	0.951	131.80	29.00	314.80	0.16	-0.61	294.52	21.19	41.8	-13.1	64.4
1852K1	-	1.000	0.905	131.12	37.21	319.27	0.19	-	292.74	27.10	39.6	-13.8	64.5
IAU_RER	26.40	0.965	0.951	131.80	29.00	314.80	0.19	-0.72	298.60	13.32	44.1	-5.6	66.8
2013UQ4	60.57	0.982	1.081	145.26	23.31	317.66	0.27	-0.97	298.16	13.03	44.8	-9.5	65.9
273P	32.83	0.975	0.810	136.40	20.19	320.43	0.28	-0.65	305.52	13.77	42.0	-4.9	67.6
2023_THC	7.68	0.923	0.589	136.73	82.55	318.55	0.00	0.00	238.73	42.81	28.5	-10.1	61.7
IAU_FSO	4.67	0.898	0.475	136.00	84.50	319.00	0.12	0.52	236.62	43.75	258.3	-4.0	61.2
IAU_THC	16.10	0.969	0.499	138.00	92.00	317.00	0.20	-0.32	224.31	41.97	23.0	-10.2	61.8
1939H1	62.17	0.992	0.528	138.17	89.15	312.35	0.22	-0.59	223.49	41.83	21.9	-10.3	62.1
2023_NFC	14.47	0.932	0.985	135.56	343.89	302.82	0.00	-0.50	314.47	-11.20	44.2	-10.3	65.0
IAU_NFC	9.08	0.880	0.980	144.16	339.42	311.17	0.25	-0.33	328.10	-11.88	50.7	-2.4	66.3
1110K1	-	1.000	0.830	137.00	358.00	321.00	0.28	-	300.47	-1.36	45.6	-8.1	66.7

4 Parent body

The average orbits of the four groups were compared with the IAU group and the parent body candidates (*Table 2*). The ERIs match very well, and the parent body is thought to be Comet 1852K1. The RERs seem to include some that are judged to be ERIs, and two comets are thought to be the parent bodies. THC is twinned with FSO, and both are thought to have Comet 1939H1 as parent body. For NFC, Comet 1110K1 has a slightly larger D_{sh}, but is thought to be the parent body. The high activity in 2023 is thought to be due to these four groups being active together.

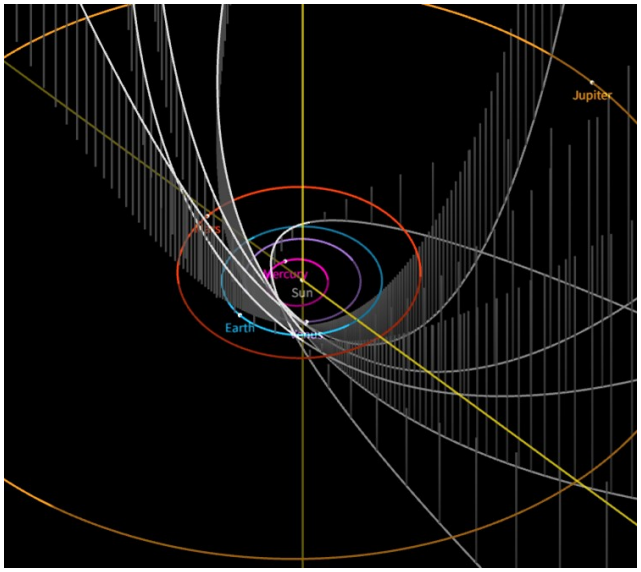

Figure 27 – Plot of the orbits of five comets.

Orbital maps of the parent comets also suggest that the activity in 2023 is due to the dust trails of these five parent comets being close to each other and active together for a long period of time (*Figure 27*).

Acknowledgment

We would like to thank the SonotaCo network for providing orbital calculation data for this study. We would also like to thank Paul Roggemans for proofreading and advice.

April 2025 CARMELO report

Mariasole Maglione[1], **Lorenzo Barbieri**[2]

[1] **Gruppo Astrofili Vicentini, Italy**
mariasole@astrofilivicentini.it

[2] **CARMELO network and AAB: Associazione Astrofili Bolognesi, Italy**
carmelometeor@gmail.com

The CARMELO network (Cheap Amateur Radio Meteor Echoes LOgger) is a collaboration of SDR radio receivers aimed at detecting meteor echoes. This report presents the data for April 2025.

1 Introduction

April is the first spring month to show prevalent meteoric showers, such as the ancient Lyrids (LYR). Peak activity for 2025 was expected between April 21 and 22. The CARMELO network observed moderate activity, with a slight increase in the night of April 22–23, at the time when the Lyrids were approximately in meridian.

2 Methods

The CARMELO network consists of SDR radio receivers. In them, a microprocessor (Raspberry) performs three functions simultaneously:

- By driving a dongle, it tunes the frequency on which the transmitter transmits and tunes like a radio, samples the radio signal and through the FFT (Fast Fourier Transform) measures frequency and received power.
- By analyzing the received data for each packet, it detects meteor echoes and discards false positives and interference.
- It compiles a file containing the event log and sends it to a server.

The data are all generated by the same standard, and are therefore homogeneous and comparable. A single receiver can be assembled with a few devices whose total current cost is about 210 euros.

To participate in the network read the instructions on this page[8].

3 April data

In the plots that follow, all available at this page[9], the abscissae represent time, which is expressed in UT (Universal Time) or in solar longitude (Solar Long), and the ordinates represent the hourly rate, calculated as the total number of events recorded by the network in an hour divided by the number of operating receivers.

In *Figure 1*, the trend of signals detected by the receivers for the month of April.

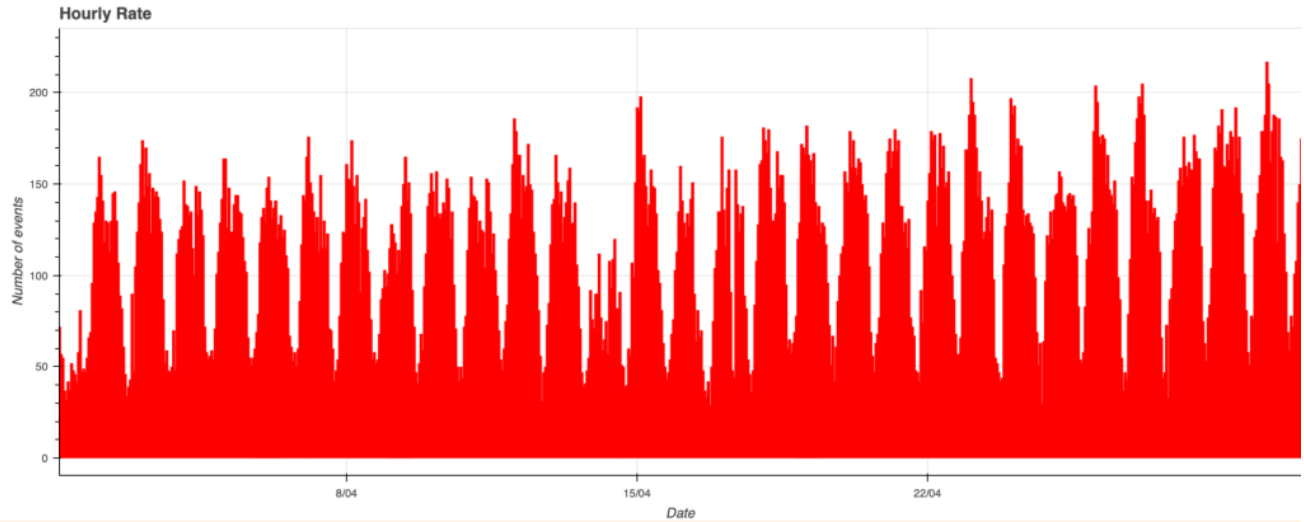

Figure 1 – April 2025 data trend.

[8] http://www.astrofiliabologna.it/about_carmelo

[9] http://www.astrofiliabologna.it/graficocarmelohr

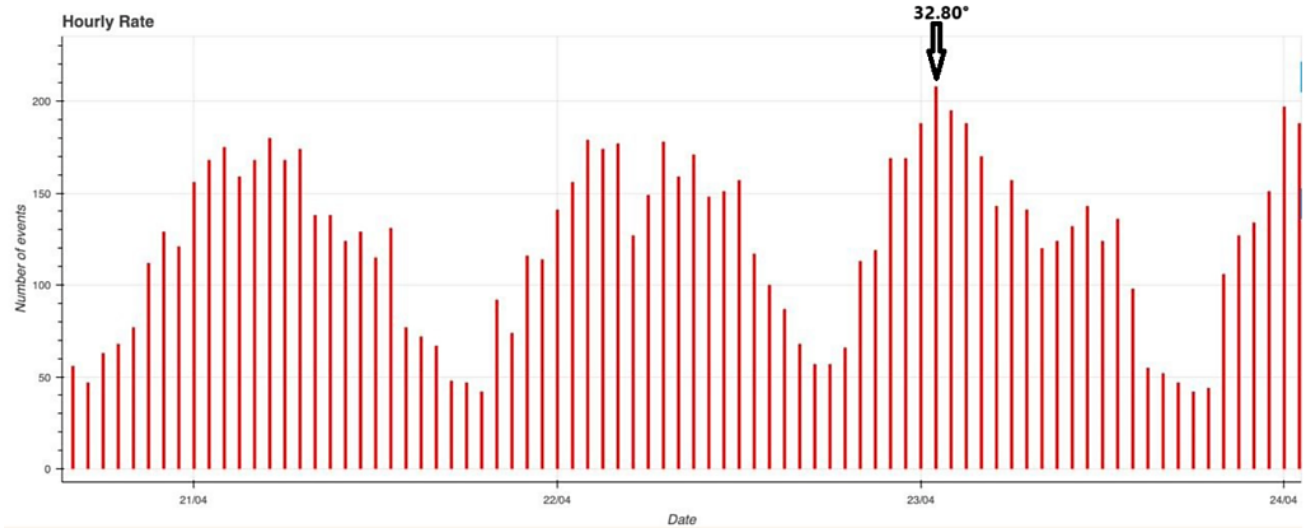

Figure 2 – Hourly rate between April 21 and 24, 2025, with a peak in meteor activity on April 23 at a solar longitude of 32.80°.

4 Lyrids

Lyrids are an annually active meteor shower in April, usually peaking around the 22nd of the month. It is one of the oldest showers ever observed, and the shower with the longest continuous historical record, with observations dating back to at least 687 B.C. (Martínez Usó et al., 2023).

The progenitor body was identified in the 19th century as comet C/1861 G1 (Thatcher), which takes about 415 years to make an orbit around the Sun. Meteors from this shower have the constellation Lyra as their radiant, near the bright star Vega. Lyrids are distinguished by their speed (about 49 km/s) and the ability to produce bright, persistent trails across the sky.

Typically, around 15–20 meteors per hour can be observed, but occasionally much higher peaks have been recorded, which were once thought to be associated with the close approach of the parent comet to Earth. However, studies conducted in the late 20th century disproved this direct correlation and suggest that outbursts may instead be linked to dynamical resonances or dense regions of material within the comet's trail (Martínez Usó et al., 2023).

One of the most intense events was the 1803 outburst, with an estimated hourly rate of about 860, which sparked great astronomical interest. A more recent one occurred in 1982, when up to 90 meteors per hour were recorded (Porubcan and Cevolani, 1985).

In 2025, the Lyrids' peak was expected during the night between April 21 and 22. The CARMELO network recorded moderate activity between April 21 and 23, with the highest detection rate on April 23, and a peak at 01^h00^m UT on April 23, at a solar longitude of 32.80°.

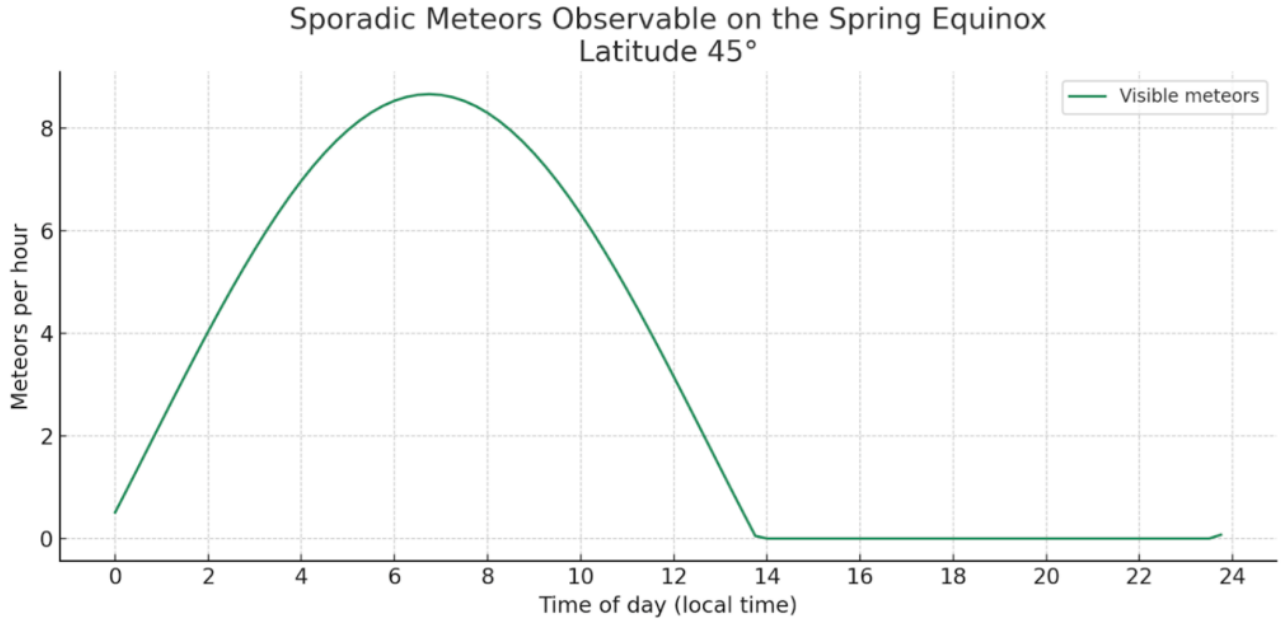

Figure 3 – Expected hourly meteor rate as a function of the time of day, near the spring equinox.

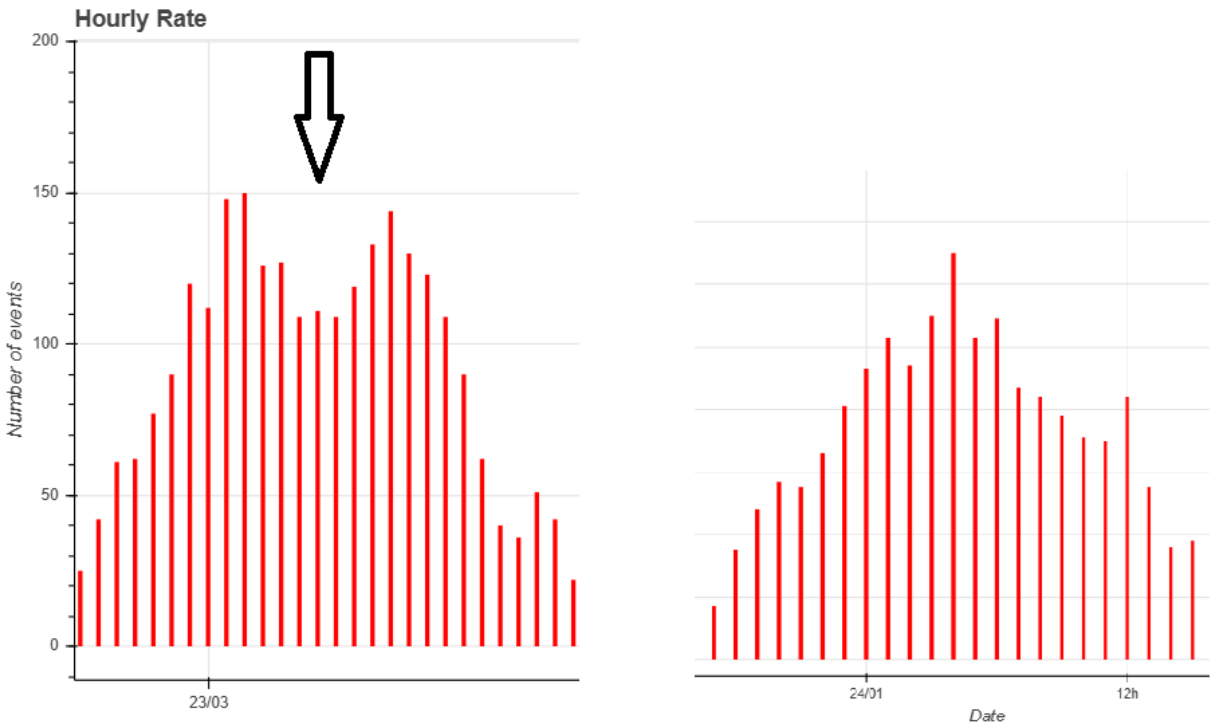

Figure 4 – On the left, hourly event rate recorded by CARMELO in April 2025, clearly showing the "6 a.m. gap"; on the right, data recorded during winter.

5 The 6 a.m. gap

A recurring anomaly in the data collected by the CARMELO network, already observed in the past with the RAMBO system, is the systematic drop in recorded meteors around 6 a.m. local time in spring—precisely when the theoretical daily maximum in meteor frequency would be expected.

This phenomenon, which we refer to as "the 6 a.m. gap" (see *Figure 4*), represents an apparent observational paradox that has an interesting explanation.

According to the model developed by Giovanni Schiaparelli in 1867 (Schiapparelli, 1867), the number of meteors observed is not constant throughout the day or the year, but follows regular variations. This occurs due to the combined motion of the Earth, which both rotates on its axis and orbits the Sun. Even if meteors were arriving uniformly from all directions in space (i.e., with an isotropic radiant distribution), the combined effect of the Earth's velocity and that of the meteoroid particles creates an illusion of concentration: meteors appear to arrive in greater numbers from a specific direction in the sky, known as the apex of the Earth's motion (see *Figure 5*).

This point moves across the sky each day in a path similar to that of the Sun and reaches the local meridian around 6 a.m. (true solar time), thereby generating a daily maximum in observed meteor frequency. Symmetrically, the minimum occurs around 6 p.m.

Throughout the year, the apex moves along the ecliptic, oscillating in height above the horizon: it reaches its maximum values in spring and minimum values in autumn. Thus, in spring, the apex is at high altitudes (70–80° above the horizon) during its morning meridian transit.

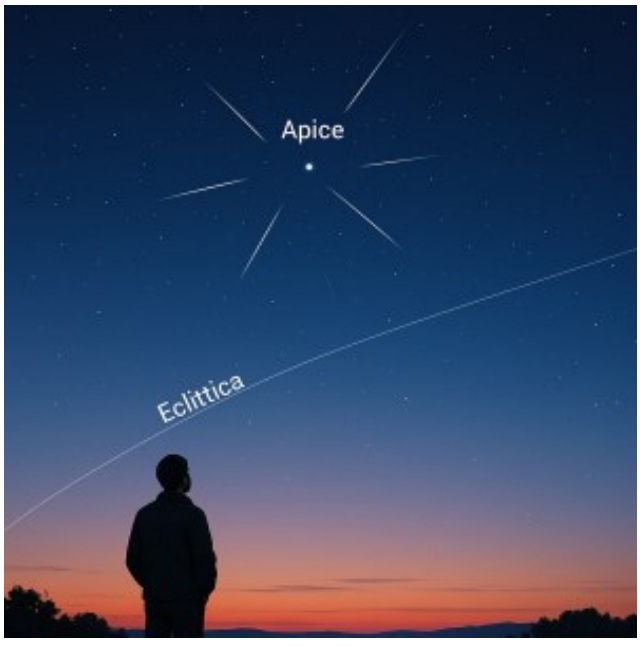

Figure 5 – Representation of the apex of Earth's motion relative to the ecliptic and the position of an observer on Earth.

The antennas used in the CARMELO network are characterized by moderate directivity and, being fixed, have maximum gain concentrated in a specific portion of the sky.

Specifically, the area where the antenna is most sensitive to radio signals reflected by meteors generally corresponds to heights above the horizon between +30° and +40° above the horizon.

As a result, the network's antennas are less sensitive to meteors occurring at very high altitudes in the sky. Consequently, when the apex of Earth's motion culminates at high heights above the horizon (see *Figure 7*), as it does in spring around 6 a.m., meteors arriving from that direction are detected less effectively, leading to a decrease in recorded events precisely when, geometrically, the highest activity would be expected.

This effect is more evident in spring for two main reasons:

- The apex reaches higher heights above the horizon.
- Meteor activity is dominated by sporadic meteors, which makes the sinusoidal pattern "cleaner" and more distinguishable.

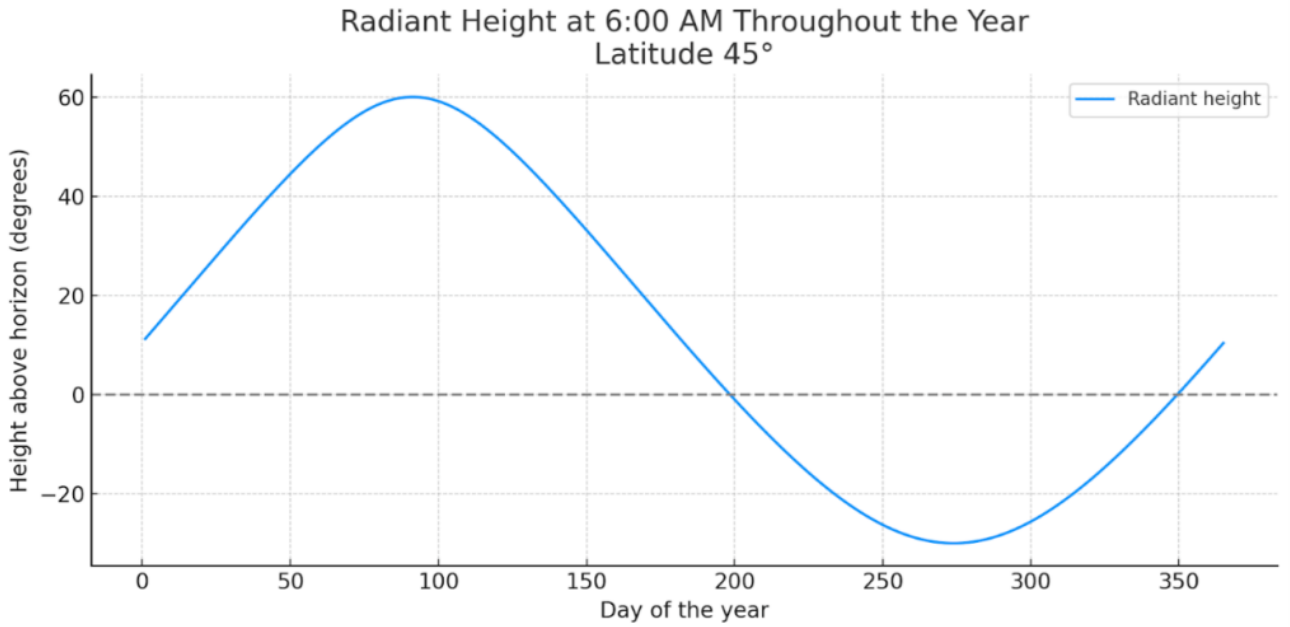

Figure 6 – Annual trend of the radiant's altitude above the horizon.

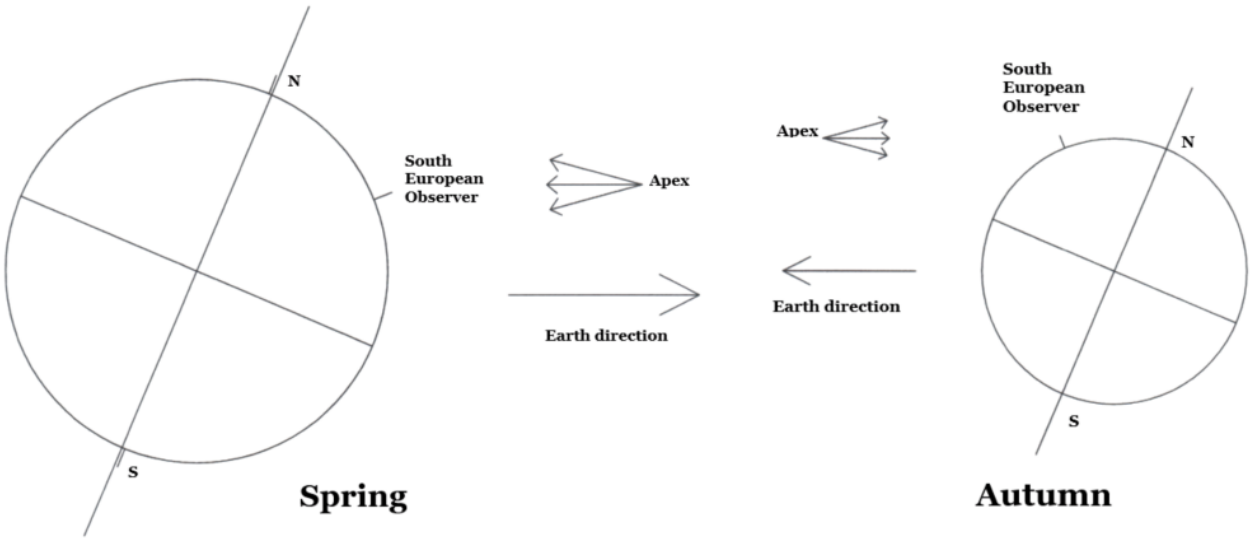

Figure 7 – Position of the apex of Earth's motion in spring and autumn.

6 The CARMELO network

The network currently consists of 14 receivers, 13 of which are operational, located in Italy, the UK, Croatia and the USA. The European receivers are tuned to the Graves radar station frequency in France, which is 143.050 MHz. Participating in the network are:

- Lorenzo Barbieri, Budrio (BO) ITA;
- Associazione Astrofili Bolognesi, Bologna ITA;

- Associazione Astrofili Bolognesi, Medelana (BO) ITA;
- Paolo Fontana, Castenaso (BO) ITA;
- Paolo Fontana, Belluno (BL) ITA;
- Associazione Astrofili Pisani, Orciatico (PI) ITA;
- Gruppo Astrofili Persicetani, San Giovanni in Persiceto (BO) ITA;
- Roberto Nesci, Foligno (PG) ITA;
- MarSEC, Marana di Crespadoro (VI) ITA;
- Gruppo Astrofili Vicentini, Arcugnano (VI) ITA;
- Associazione Ravennate Astrofili Theyta, Ravenna (RA) ITA;
- Akademsko Astronomsko Društvo, Rijeka CRO;
- Mike German a Hayfield, Derbyshire UK;
- Mike Otte, Pearl City, Illinois USA.

The authors' hope is that the network can expand both quantitatively and geographically, thus allowing the production of better-quality data.

References

Martínez Usó M. J., Marco Castillo F. J., López Ortí J. A. (2023). "The Lyrids meteor shower: A historical perspective". *Planetary and Space Science*, **238**, article id. 105803.

Porubcan V., Cevolani G. (1985). "Unusual Display of the Lyrid Meteor Shower in 1982". *Contributions of the Astronomical Observatory Skalnate Pleso*, **13**, 247–253.

Giovanni Schiapparelli (1867). Teoria astronomica delle stelle cadenti, Columbia University Press.

May 2025 CARMELO report

Mariasole Maglione[1], **Lorenzo Barbieri**[2], **Silvana Sarto**[2]

[1] **Gruppo Astrofili Vicentini, Italy**
mariasole@astrofilivicentini.it

[2] **CARMELO network and AAB: Associazione Astrofili Bolognesi, Italy**
carmelometeor@gmail.com

The CARMELO network (Cheap Amateur Radio Meteor Echoes LOgger) is a collaboration of SDR radio receivers aimed at detecting meteor echoes. This report presents the data for May 2025.

1 Introduction

In May, the CARMELO network did not detect particularly intense meteor activity. Early in the month there was a peak, though not very pronounced, of the Eta Aquariids (ETA) shower on the night of May 5–6. We also report the detection of a meteor outburst probably related to comet 73P/Schwassmann-Wachmann in early June.

2 Methods

The CARMELO network consists of SDR radio receivers. In them, a microprocessor (Raspberry) performs three functions simultaneously:

- By driving a dongle, it tunes the frequency on which the transmitter transmits and tunes like a radio, samples the radio signal and through the FFT (Fast Fourier Transform) measures frequency and received power.
- By analyzing the received data for each packet, it detects meteor echoes and discards false positives and interference.
- It compiles a file containing the event log and sends it to a server.

The data are all generated by the same standard, and are therefore homogeneous and comparable. A single receiver can be assembled with a few devices whose total current cost is about 210 euros.

To participate in the network read the instructions on this page[10].

3 May data

In the plots that follow, all available online[11], the abscissae represent time, which is expressed in UT (Universal Time) or in solar longitude (Solar Long), and the ordinates represent the hourly rate, calculated as the total number of events recorded by the network in an hour divided by the number of operating receivers.

In *Figure 1*, the trend of signals detected by the receivers for the month of May.

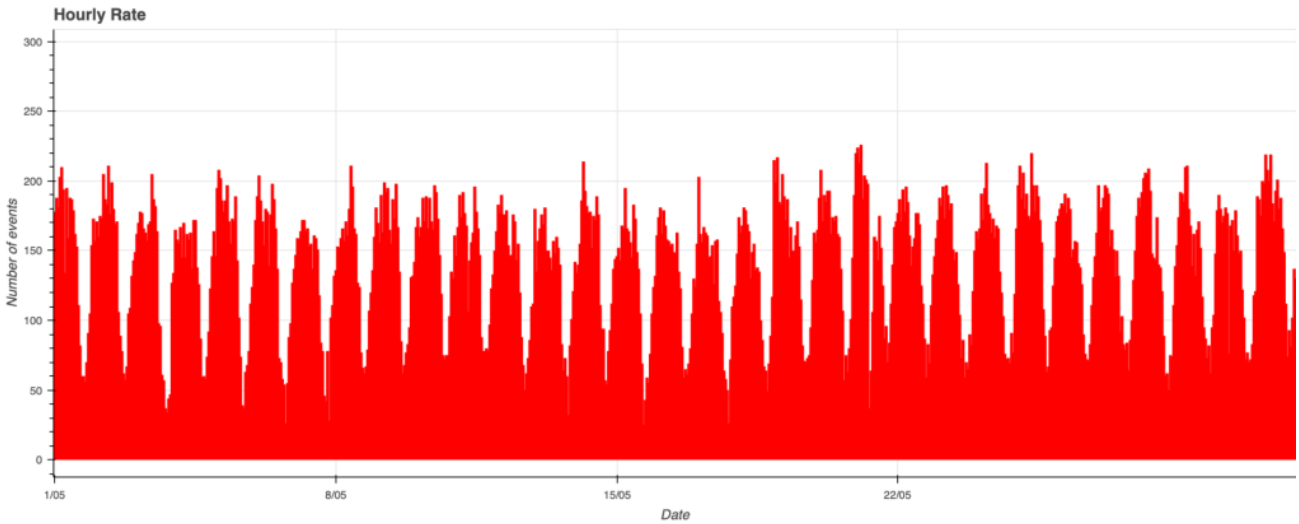

Figure 1 – May 2025 data trend.

[10] http://www.astrofiliabologna.it/about_carmelo

[11] http://www.astrofiliabologna.it/graficocarmelohr

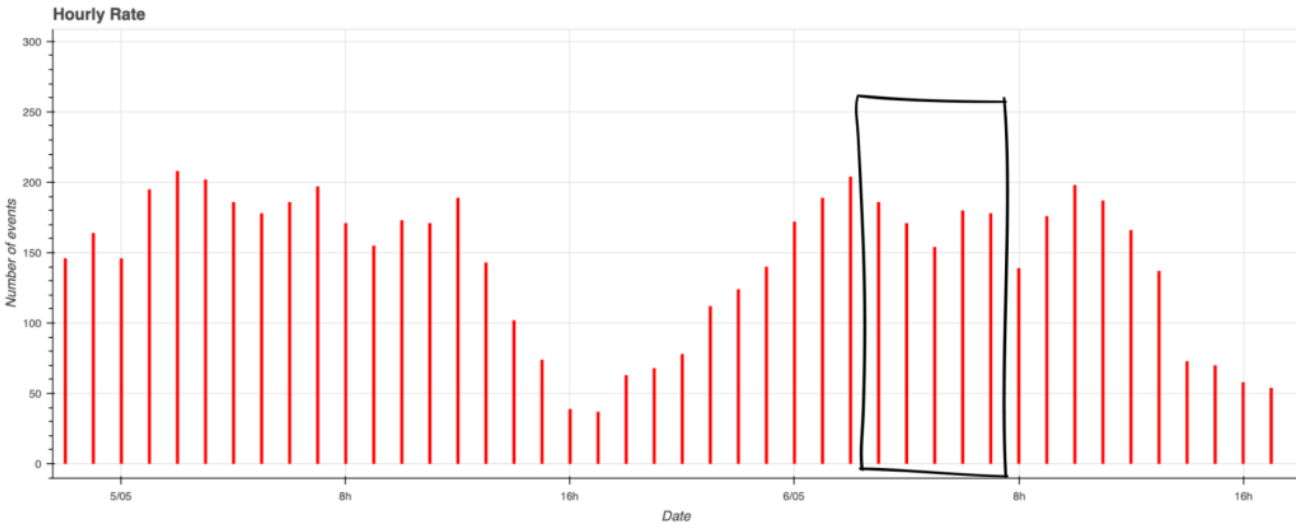

Figure 2 – Hourly rate between May 5 and 6, 2025, with very moderate meteor activity.

4 Eta Aquariids

Eta Aquariids (ETAs) are a meteor shower active every year between mid-April and late May, with a peak visibility around May 6. Although less conspicuous than better-known showers, the Eta Aquariids are of some special importance because of their origin: their fragments come from the famous Halley's comet, the same comet that also gives rise to the Orionids in October (Egal et al., 2020).

The radiant of the shower is located in the constellation Aquarius, near the star Eta Aquarii, from which it takes its name. In our latitudes this point rises just before sunrise, around 3^h30^m a.m., making the last hours of the night the most suitable time for observation and detection. Because of the radiant's low position on the horizon, the number of meteors visible in Italy is generally limited to about 30 to 40 per hour. In the southern regions, where the radiant rises much higher on the horizon, the shower instead offers a far more intense show, with hourly rates at zenith (ZHR) that can exceed 50–60 meteors per hour.

Eta Aquariids are also distinguished by the high speed of the meteors, which can reach over 66 km/s. This makes their tracks in the sky particularly bright and persistent, with trails that sometimes persist for several seconds.

In 2025, the peak in the shower's activity was expected on the night of May 5–6. The CARMELO network recorded moderate activity, particularly between 2^h00^m a.m. and 5^h00^m a.m. on May 6, where the maximum count was 204 events at 2^h00^m a.m. when the radiant was still below the horizon, and thereafter, around dawn, it hovered between 170 and 180 events, between solar longitudes 45.55° and 45.67°.

5 The outbursts of May 31 and June 1

On June 6, the Central Bureau for Astronomical Telegrams published CBET 5561 (Vida et al., 2025), reporting two intense meteor outbursts potentially associated with the minor shower of Tau Herculids (TAH#64), generated by fragments of comet 73P/Schwassmann-Wachmann. The observations were conducted by the Global Meteor Network, which showed two distinct peaks in the hourly rate of meteors, the second of which ended abruptly around 0^h00^m UTC on June 2 (solar longitude 70.71°).

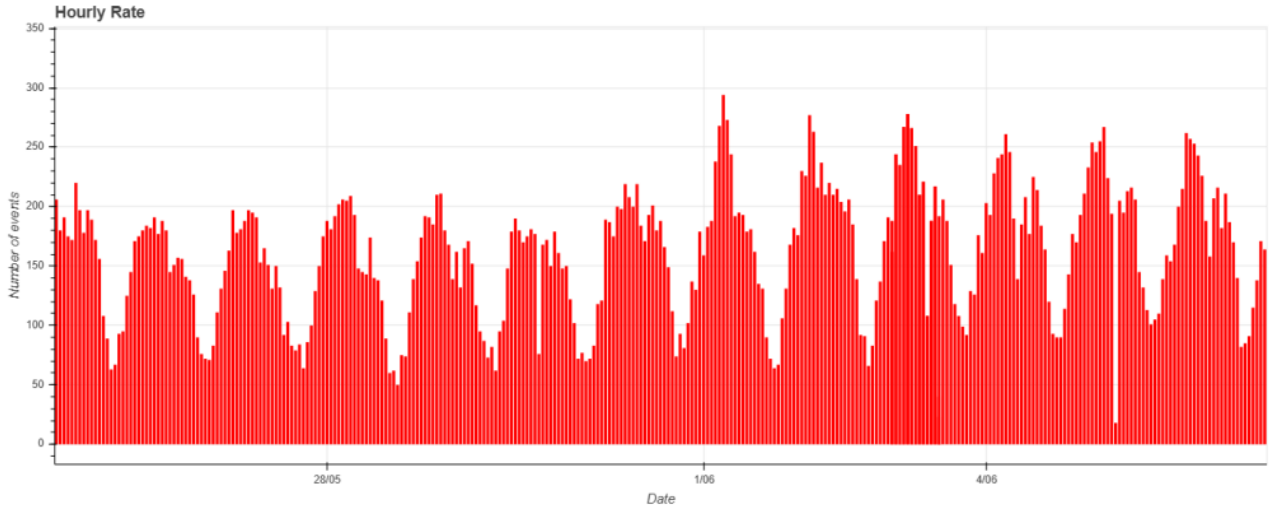

Figure 3 – Hourly rate between the end of May and the beginning of June 2025.

When a comet such as 73P/Schwassmann-Wachmann fragments (as it did spectacularly in 1995, with further ruptures observed in 2006), it releases material in large quantities: large and small fragments, dust, and meteoroids that are ejected with slightly different velocities from each other. These differences in initial velocities, even small ones, lead over time to meteoroids being distributed along the comet's orbit unevenly. This process is called differential expansion: faster particles move forward, slower particles stay behind. After years or decades, these "clouds" separate, generating packets or filaments that can intersect Earth's orbit at specific times, resulting in brief but intense meteor outbursts.

In the case of comet 73P, several modeling studies (Egal et al., 2023) predicted that debris ejected in the 1995 and 2006 passages-key years for its breakup events-might have reached Earth around 2022–2025. The behavior observed these days is consistent with the arrival of one of these meteoroid filaments, confirming the simulations.

Looking at the data from the CARMELO network, we indeed notice an increase in the number of meteor echoes detected between June 1 and June 2, followed by a sudden decrease right at solar longitude 70.71° as indicated in CBET.

The shower's radiant associated with comet 73P was transiting the meridian right around midnight. This means that no significant change in the observing geometry had occurred at the time of the dip. The abrupt drop in meteor activity could therefore be blamed on the cessation of the meteoroid flux.

6 The CARMELO network

The network currently consists of 14 receivers, 13 of which are operational, located in Italy, the UK, Croatia and the USA. The European receivers are tuned to the Graves radar station frequency in France, which is 143.050 MHz. Participating in the network are:

- Lorenzo Barbieri, Budrio (BO) ITA;
- Associazione Astrofili Bolognesi, Bologna ITA;
- Associazione Astrofili Bolognesi, Medelana (BO) ITA;
- Paolo Fontana, Castenaso (BO) ITA;
- Paolo Fontana, Belluno (BL) ITA;
- Associazione Astrofili Pisani, Orciatico (PI) ITA;
- Gruppo Astrofili Persicetani, San Giovanni in Persiceto (BO) ITA;
- Roberto Nesci, Foligno (PG) ITA;
- MarSEC, Marana di Crespadoro (VI) ITA;
- Gruppo Astrofili Vicentini, Arcugnano (VI) ITA;
- Associazione Ravennate Astrofili Theyta, Ravenna (RA) ITA;
- Akademsko Astronomsko Društvo, Rijeka CRO;
- Mike German a Hayfield, Derbyshire UK;
- Mike Otte, Pearl City, Illinois USA.

The authors' hope is that the network can expand both quantitatively and geographically, thus allowing the production of better-quality data.

Expanding an observation network such as CARMELO (Barbieri, 2024), in fact, is crucial to improving the quality and quantity of data collected. First and foremost, increasing the number of receivers allows for greater continuity in recording events, reducing the risk of signal loss due to technical failures or local outages.

However, the real quantum leap is achieved with a wider geographic distribution. When receivers are located in different areas far apart, data can be compared and meteor trajectories can be reconstructed more accurately. An extended network also allows simultaneous events to be detected from multiple vantage points, strengthening the scientific validity of observations. Going forward, global coverage may prove essential for detecting rare transient phenomena, capturing unexpected meteor showers, and providing data to support other monitoring tools.

Finally, engaging new observatories in different regions also means strengthening international collaboration and expanding public participation in scientific research.

References

Barbieri L. (2024). "What CARMELO can observe". *eMetN Meteor Journal*, **9**, 241–248.

Egal A., Brown P. G., Rendtel J., Campbell-Brown M. and Wiegert P. (2020). "Aquariid and Orionid meteor showers". *Astronomy & Astrophysics*, **640**, A58.

Egal A., Wiegert P.A., Brown P.G., and Vida D. (2023). "Modelling the 2022 τ-Herculid outburst". *The Astrophysical Journal*, **949**, id.96, 18 pp.

Vida D., Brown P., and Egal A. (2025). "Two meteor shower outbursts with potential connection to comet 73P". Central Bureau for Astronomical Telegrams, CBET 5561.

Radio meteors April 2025

Felix Verbelen

Vereniging voor Sterrenkunde & Volkssterrenwacht MIRA, Grimbergen, Belgium
felix.verbelen@gmail.com

An overview of the radio observations during April is given.

1 Introduction

The graphs show both the daily totals (*Figure 1 and 2*) and the hourly numbers (*Figure 3 and 4*) of "all" reflections counted automatically, and of manually counted "overdense" reflections, overdense reflections longer than 10 seconds and longer than 1 minute, as observed here at Kampenhout (BE) on the frequency of our VVS-beacon (49.99 MHz) during the month of April 2025.

The hourly numbers, for echoes shorter than 1 minute, are weighted averages derived from:

$$N(h) = \frac{n(h-1)}{4} + \frac{n(h)}{2} + \frac{n(h+1)}{4}$$

Local interference was minimal during this month and no lightning activity was recorded. However, quite strong solar type III eruptions were observed on several days.

Meteor activity was generally low but increased towards the end of the month.

As expected, the Lyrids reached their peak on April 22nd, as evidenced by the counts of overdense reflections.

Six reflections exceeding one minute in duration were recorded over the entire month.

A selection of these, along with a few other interesting recordings is included (*Figures 5 to 18*).

In addition to the usual graphs, you will also find the raw counts in cvs-format[12] from which the graphs are derived. The table contains the following columns: day of the month, hour of the day, day + decimals, solar longitude (epoch J2000), counts of "all" reflections, overdense reflections, reflections longer than 10 seconds and reflections longer than 1 minute, the numbers being the observed reflections of the past hour.

[12] https://www.emeteornews.net/wp-content/uploads/2025/05/202504_49990_FV_rawcounts.csv

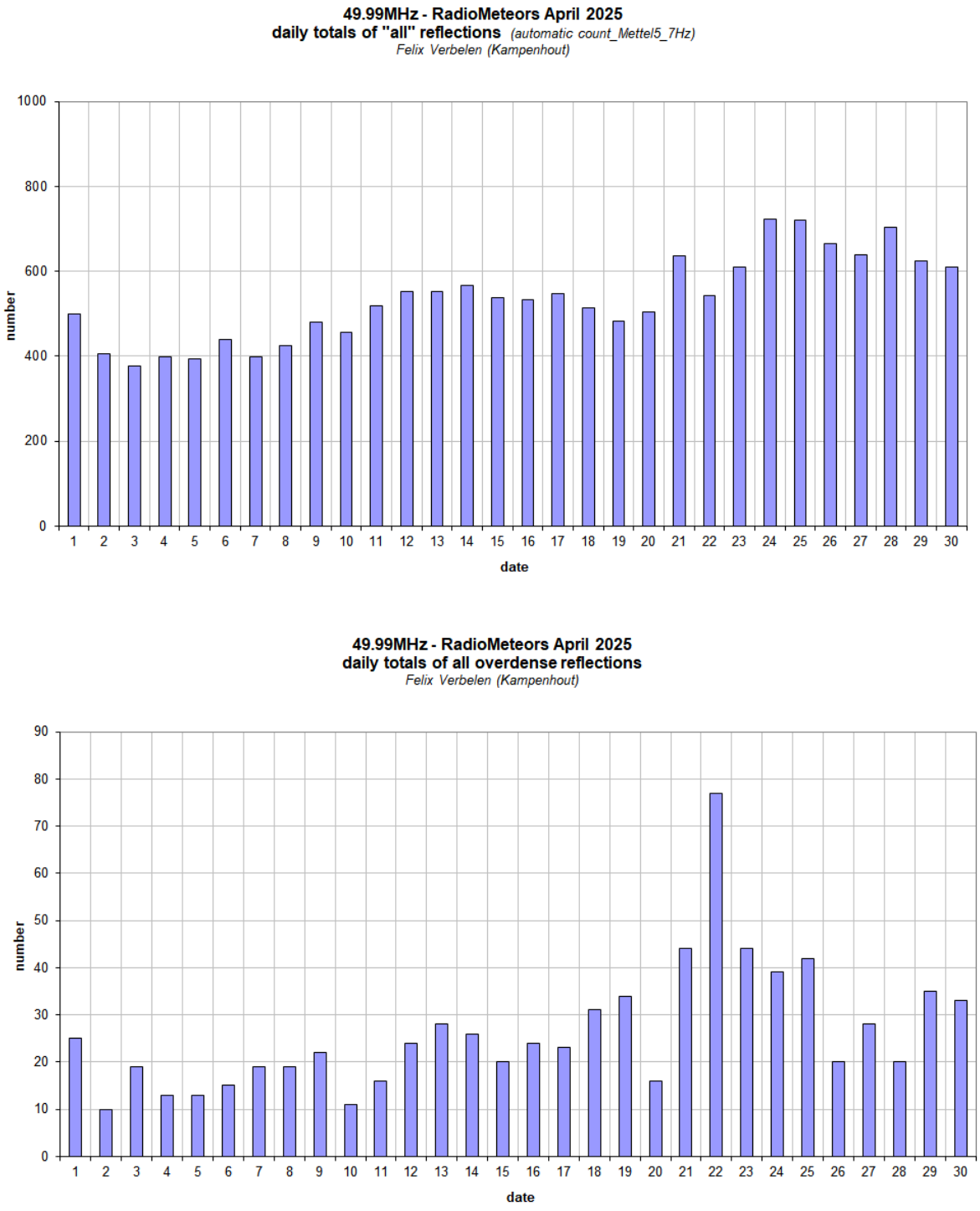

Figure 1 – The daily totals of "all" reflections counted automatically, and of manually counted "overdense" reflections, as observed here at Kampenhout (BE) on the frequency of our VVS-beacon (49.99 MHz) during April 2025.

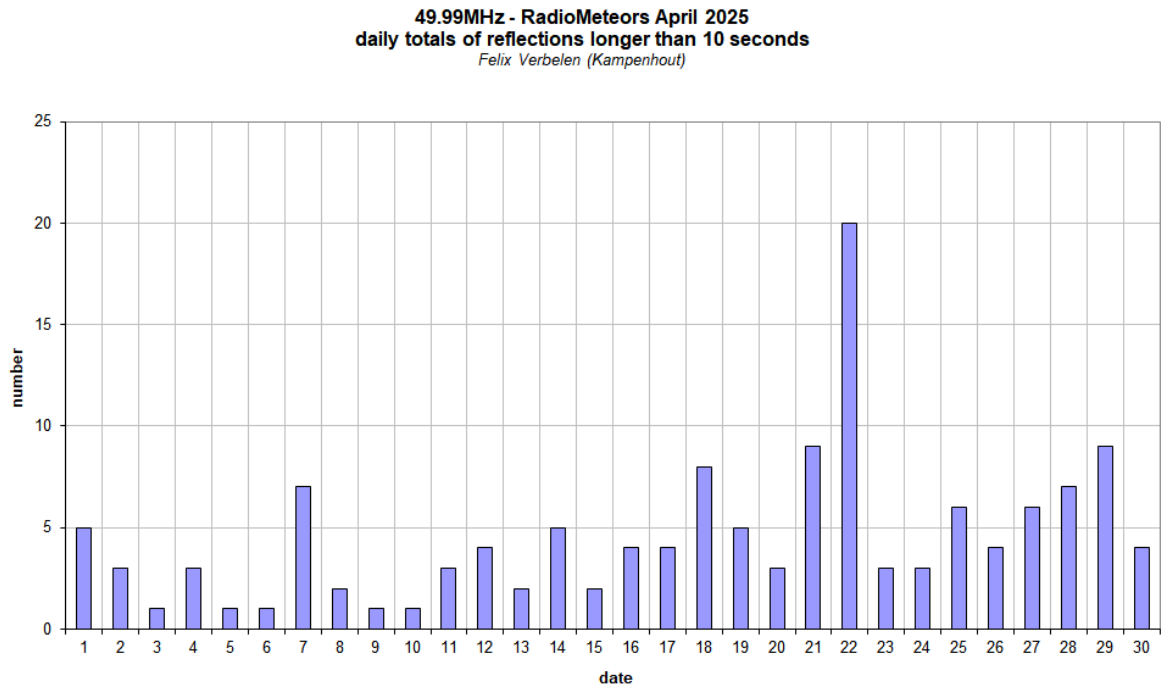

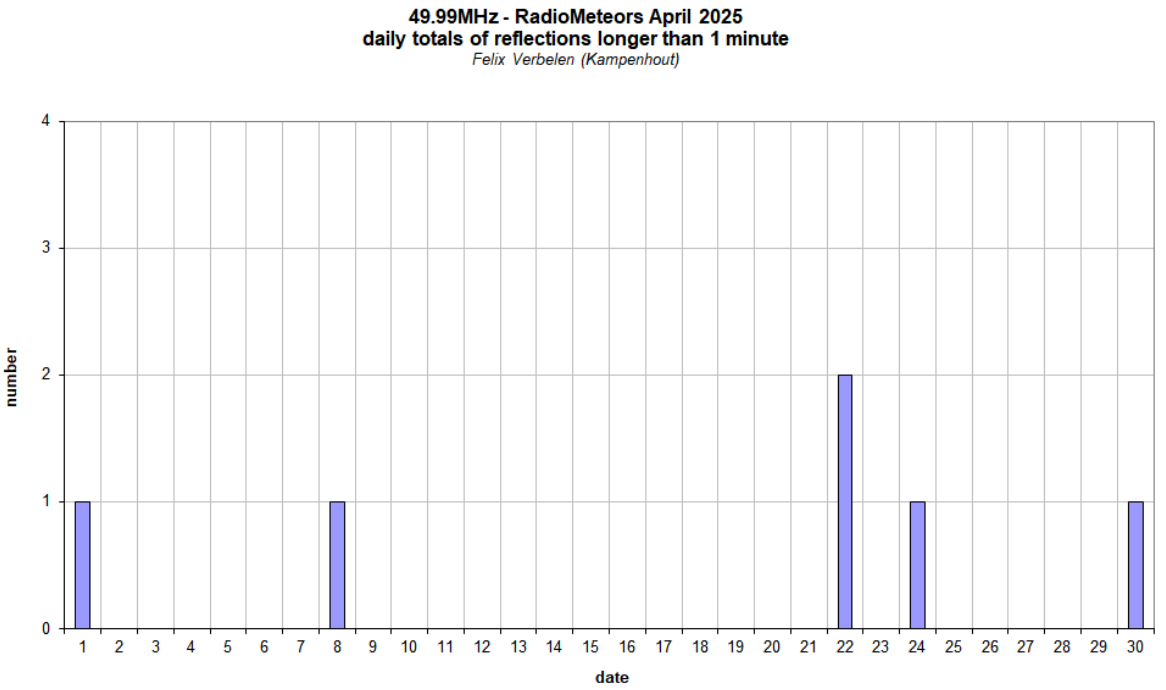

Figure 2 – The daily totals of overdense reflections longer than 10 seconds and longer than 1 minute, as observed here at Kampenhout (BE) on the frequency of our VVS-beacon (49.99 MHz) during April 2025.

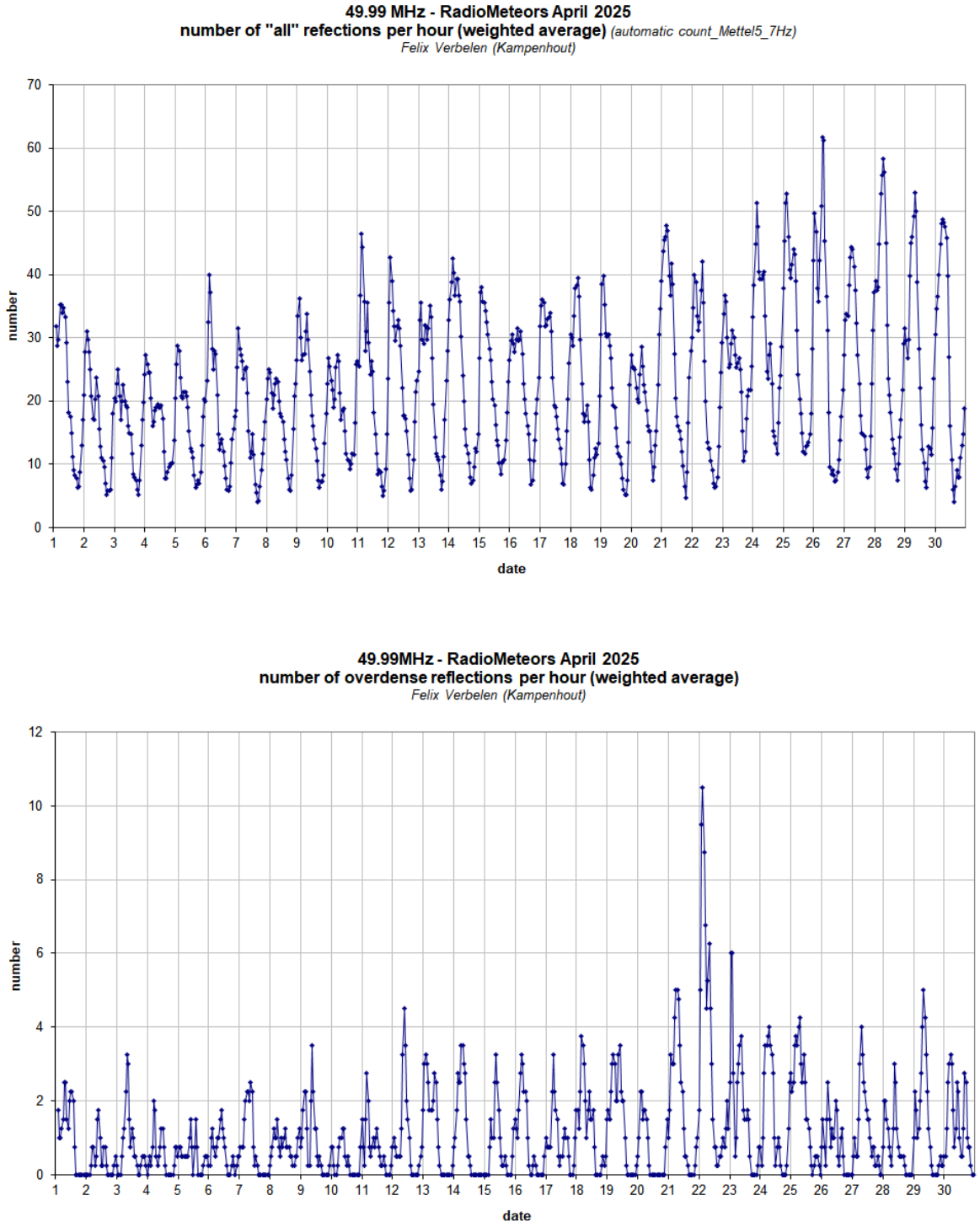

Figure 3 – The hourly numbers of "all" reflections counted automatically, and of manually counted "overdense" reflections, as observed here at Kampenhout (BE) on the frequency of our VVS-beacon (49.99 MHz) during April 2025.

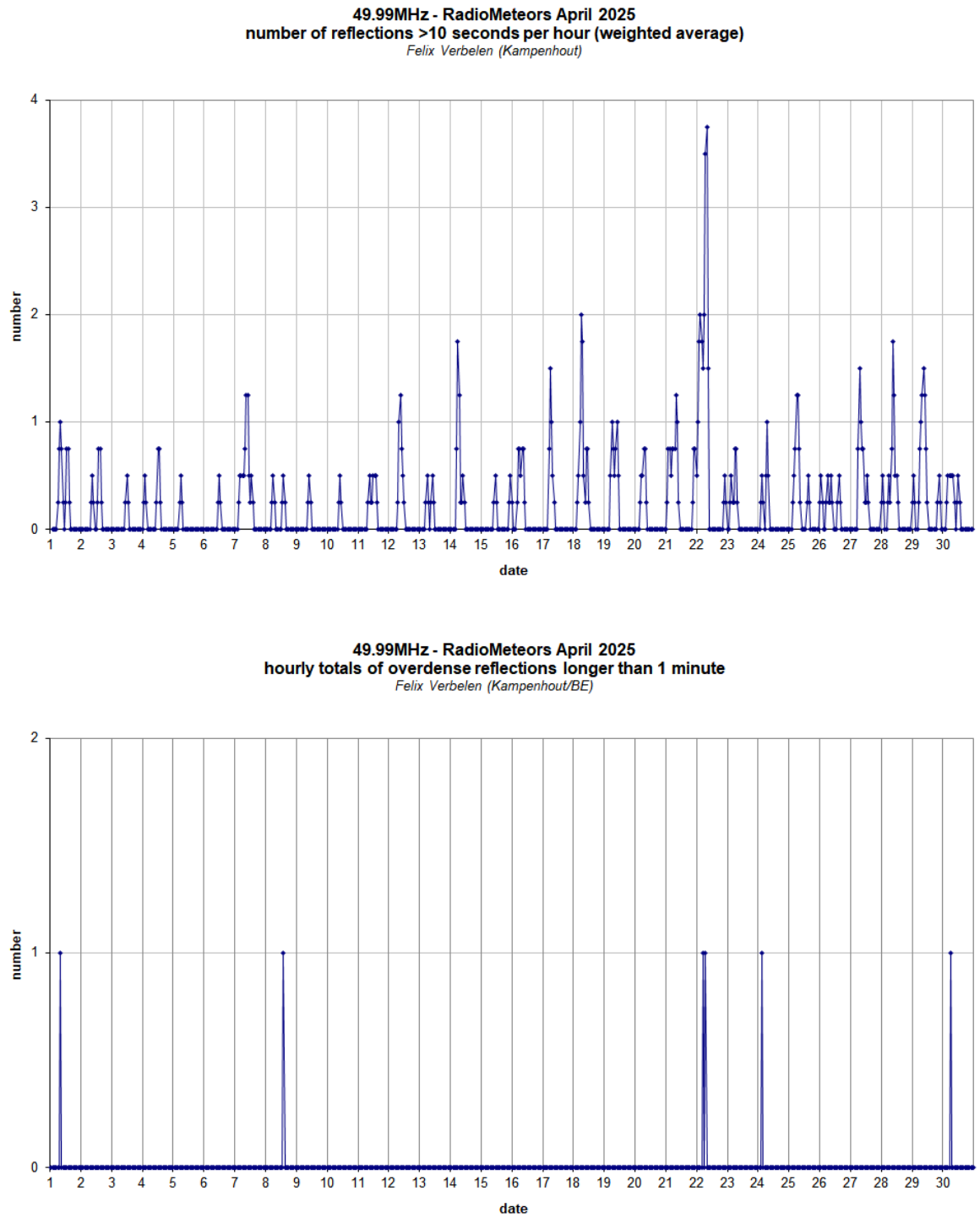

Figure 4 – The hourly numbers of overdense reflections longer than 10 seconds and longer than 1 minute, as observed here at Kampenhout (BE) on the frequency of our VVS-beacon (49.99 MHz) during April 2025.

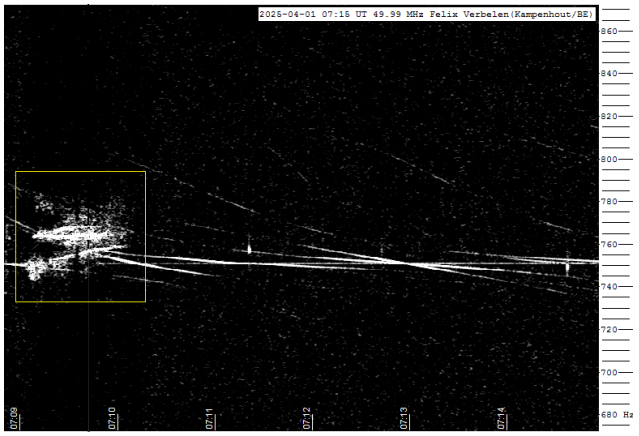

Figure 5 – Meteor echoes April 1, 7^h15^m UT.

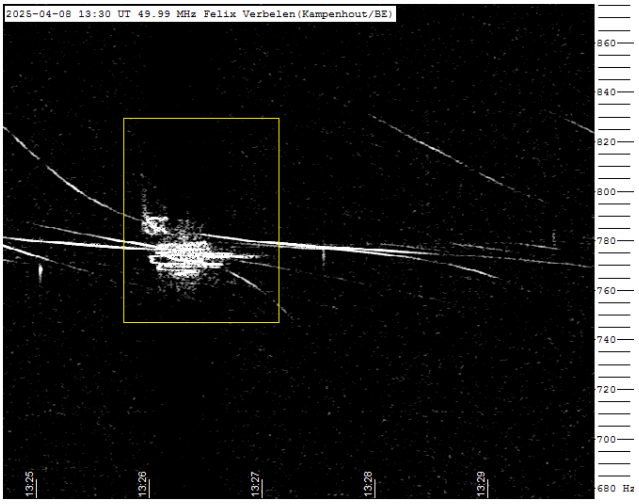

Figure 6 – Meteor echoes April 8, 13^h30^m UT.

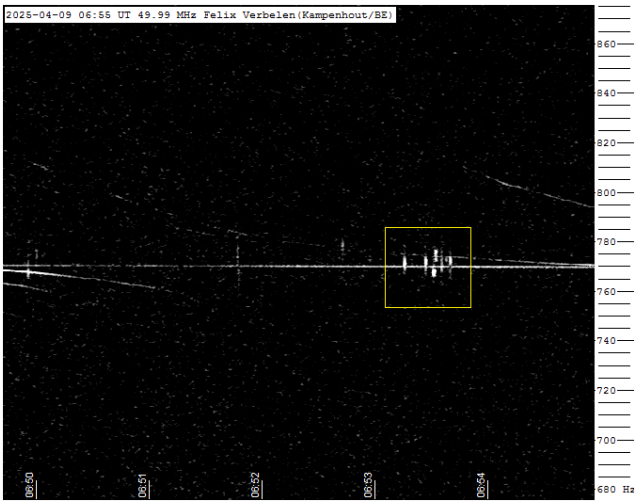

Figure 7 – Meteor echoes April 9, 6^h55^m UT.

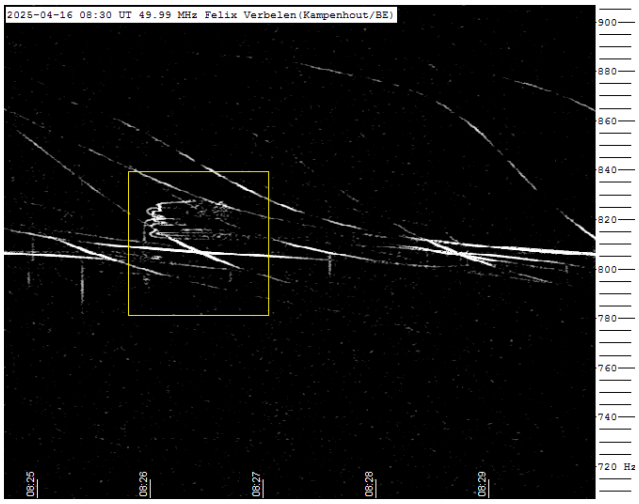

Figure 8 – Meteor echoes April 16, 8^h30^m UT.

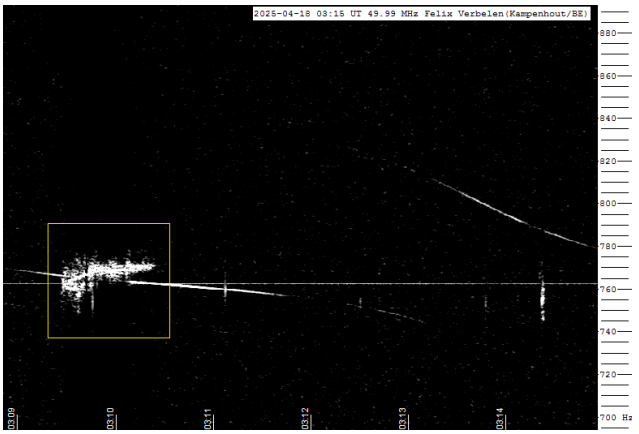

Figure 9 – Meteor echoes April 18, 3^h15^m UT.

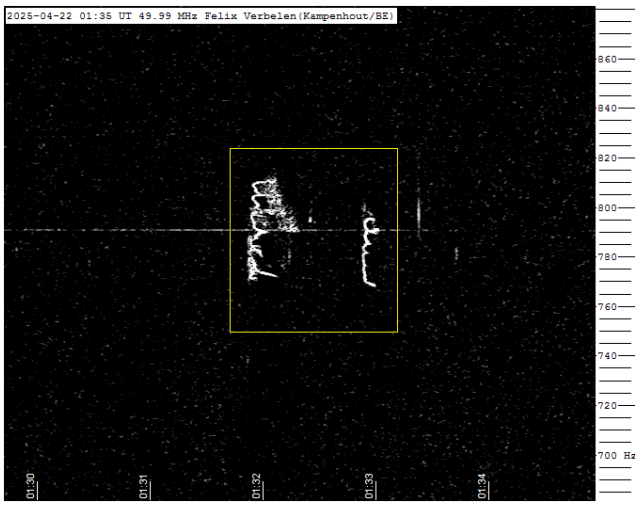

Figure 10 – Meteor echoes April 22, 1^h35^m UT.

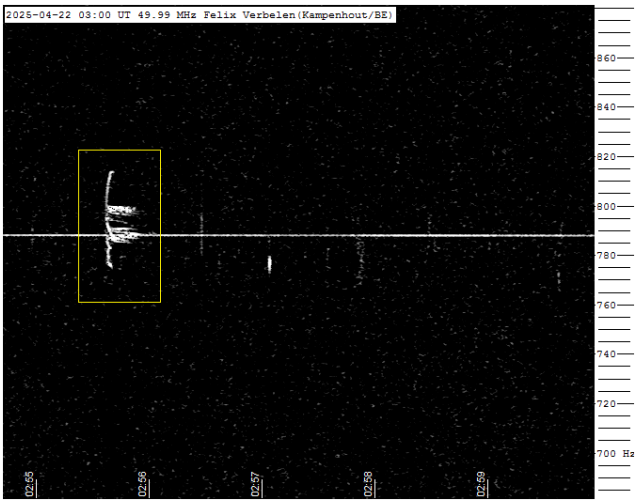

Figure 11 – Meteor echoes April 22, 3^h00^m UT.

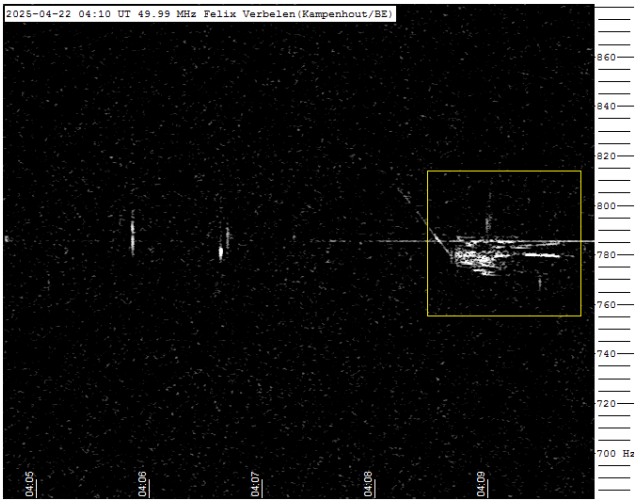

Figure 12 – Meteor echoes April 22, 4^h10^m UT.

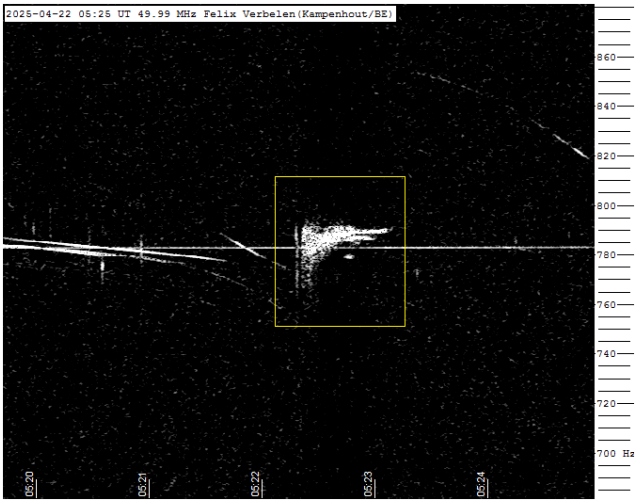

Figure 13 – Meteor echoes April 22, 5^h25^m UT.

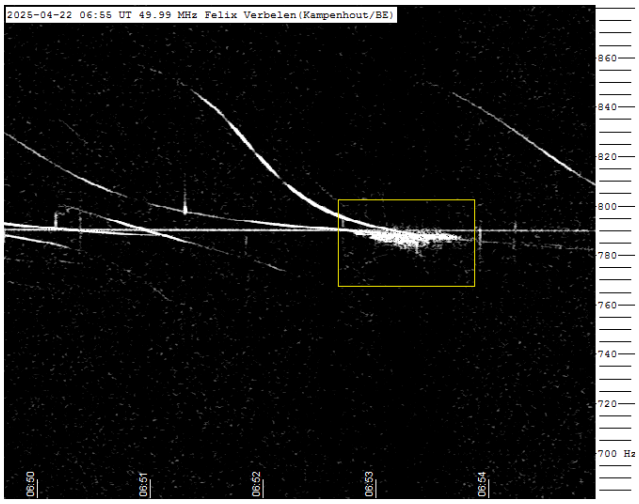

Figure 14 – Meteor echoes April 22, 6^h55^m UT.

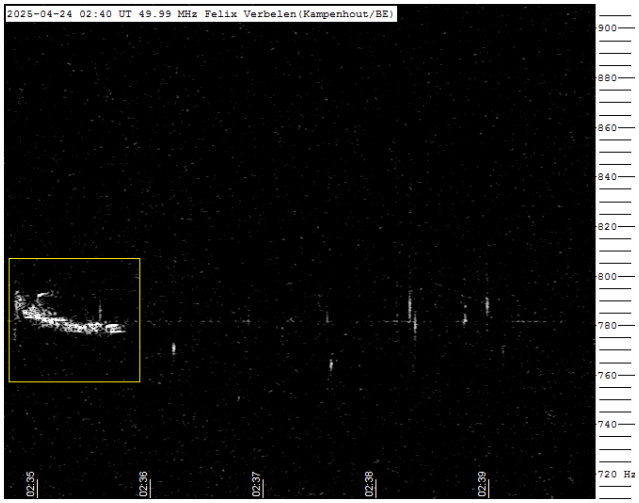

Figure 15 – Meteor echoes April 24, 2^h40^m UT.

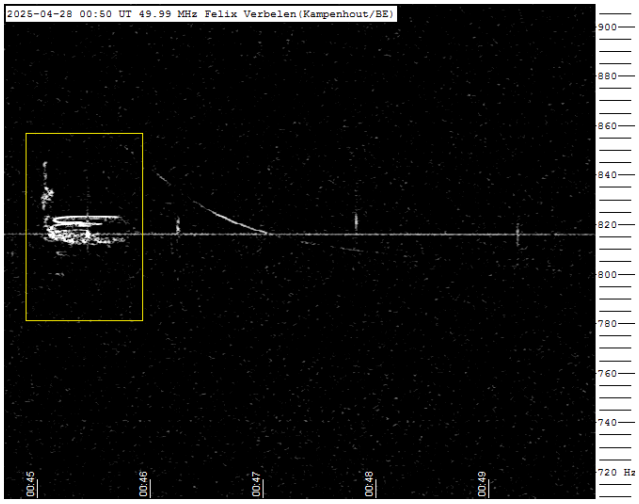

Figure 16 – Meteor echoes April 28, 0^h50^m UT.

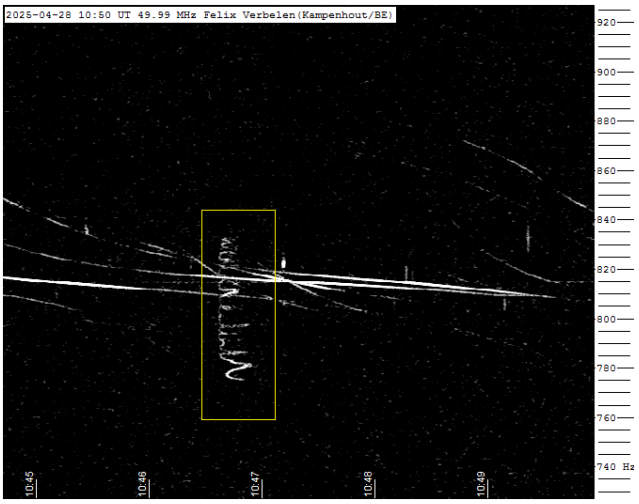

Figure 17 – Meteor echoes April 28, 10^h50^m UT.

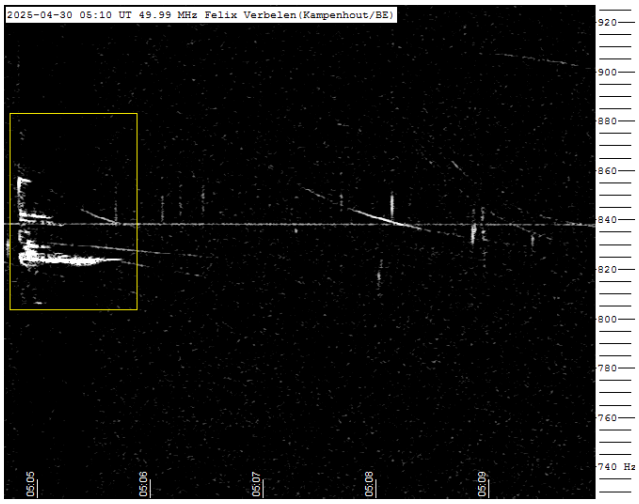

Figure 18 – Meteor echoes April 30, 5^h10^m UT.

Radio meteors May 2025

Felix Verbelen

Vereniging voor Sterrenkunde & Volkssterrenwacht MIRA, Grimbergen, Belgium
felix.verbelen@gmail.com

An overview of the radio observations during May is given.

1 Introduction

The graphs show both the daily totals (*Figure 1 and 2*) and the hourly numbers (*Figure 3 and 4*) of "all" reflections counted automatically, and of manually counted "overdense" reflections, overdense reflections longer than 10 seconds and longer than 1 minute, as observed here at Kampenhout (BE) on the frequency of our VVS-beacon (49.99 MHz) during the month of May 2025.

The hourly numbers, for echoes shorter than 1 minute, are weighted averages derived from:

$$N(h) = \frac{n(h-1)}{4} + \frac{n(h)}{2} + \frac{n(h+1)}{4}$$

During this month, there were few local disturbances, with lightning activity recorded on only two days. However, fairly strong solar flares were registered almost every day, most of them Type III.

Overall, meteor activity remained weak, below the average of previous years. The number of Eta Aquariids also remained subpar, but with a clear presence during the first decade of the month, especially regarding longer reflections. Throughout the entire month, 10 reflections longer than 1 minute were recorded.

A selection of these, along with a few other interesting recordings is included (*Figures 5 to 20*).

In addition to the usual graphs, you will also find the raw counts in cvs-format[13] from which the graphs are derived. The table contains the following columns: day of the month, hour of the day, day + decimals, solar longitude (epoch J2000), counts of "all" reflections, overdense reflections, reflections longer than 10 seconds and reflections longer than 1 minute, the numbers being the observed reflections of the past hour.

[13] https://www.emeteornews.net/wp-content/uploads/2025/05/202504_49990_FV_rawcounts.csv

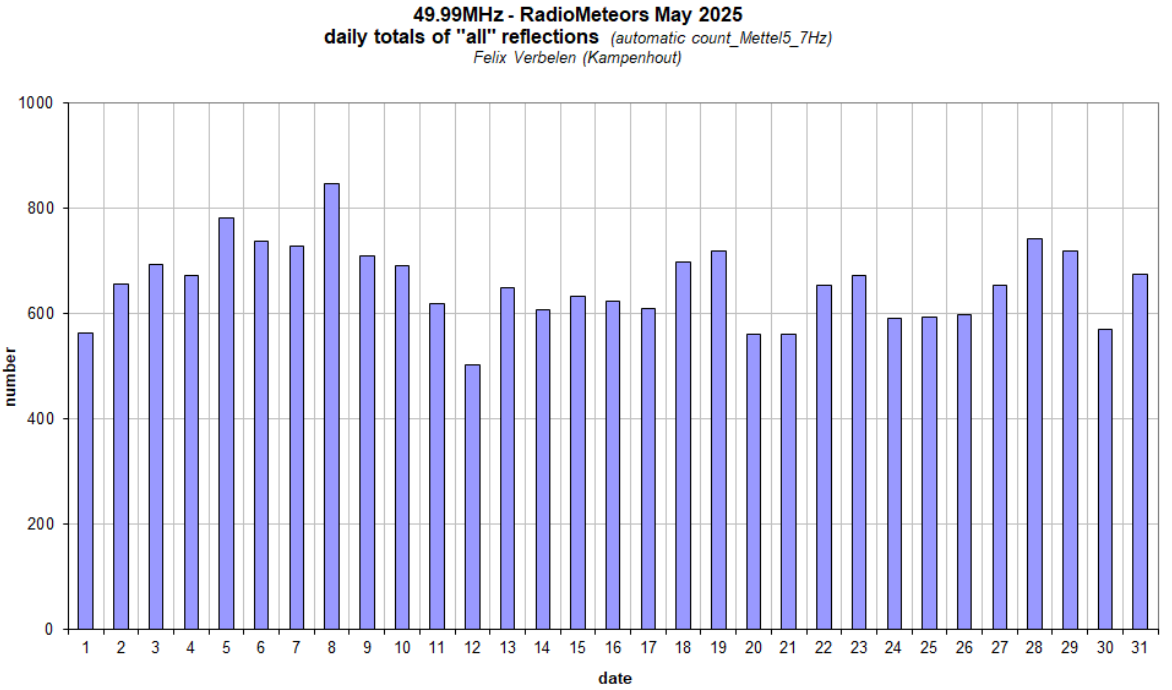

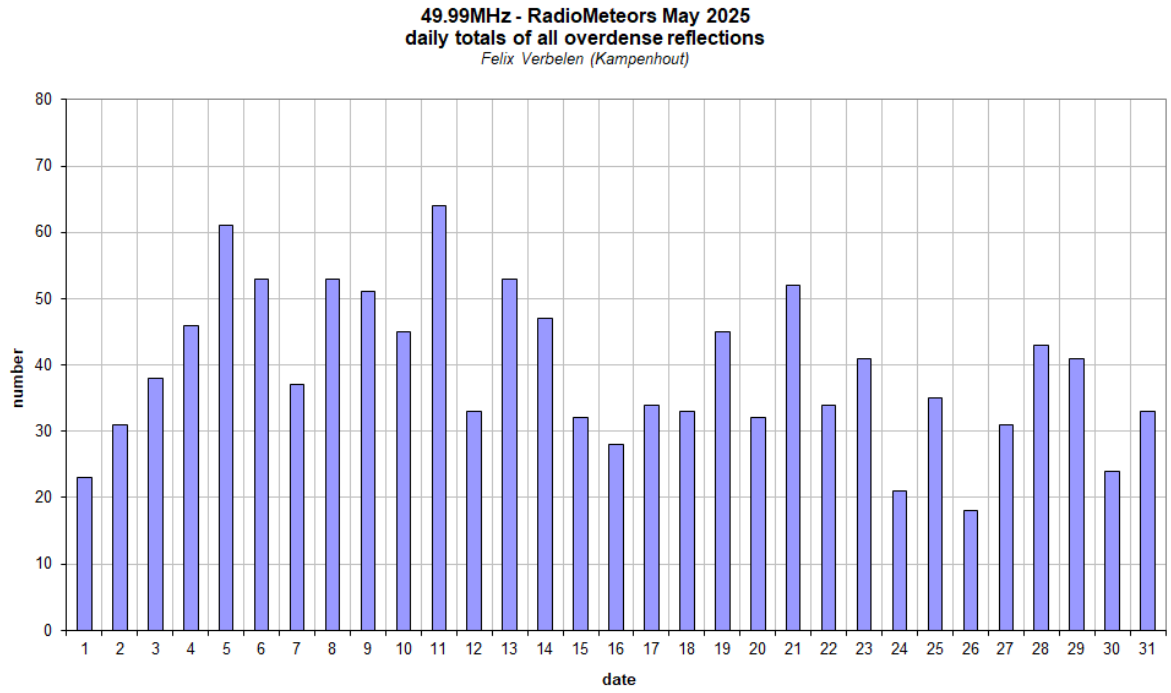

Figure 1 – The daily totals of "all" reflections counted automatically, and of manually counted "overdense" reflections, as observed here at Kampenhout (BE) on the frequency of our VVS-beacon (49.99 MHz) during May 2025.

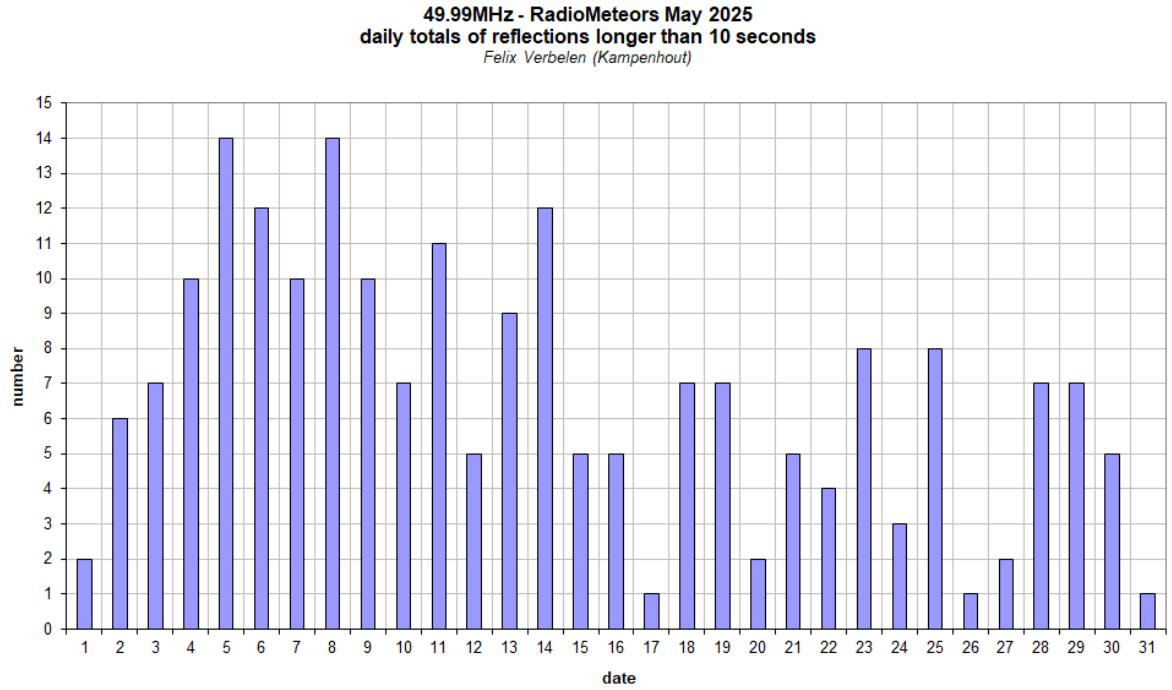

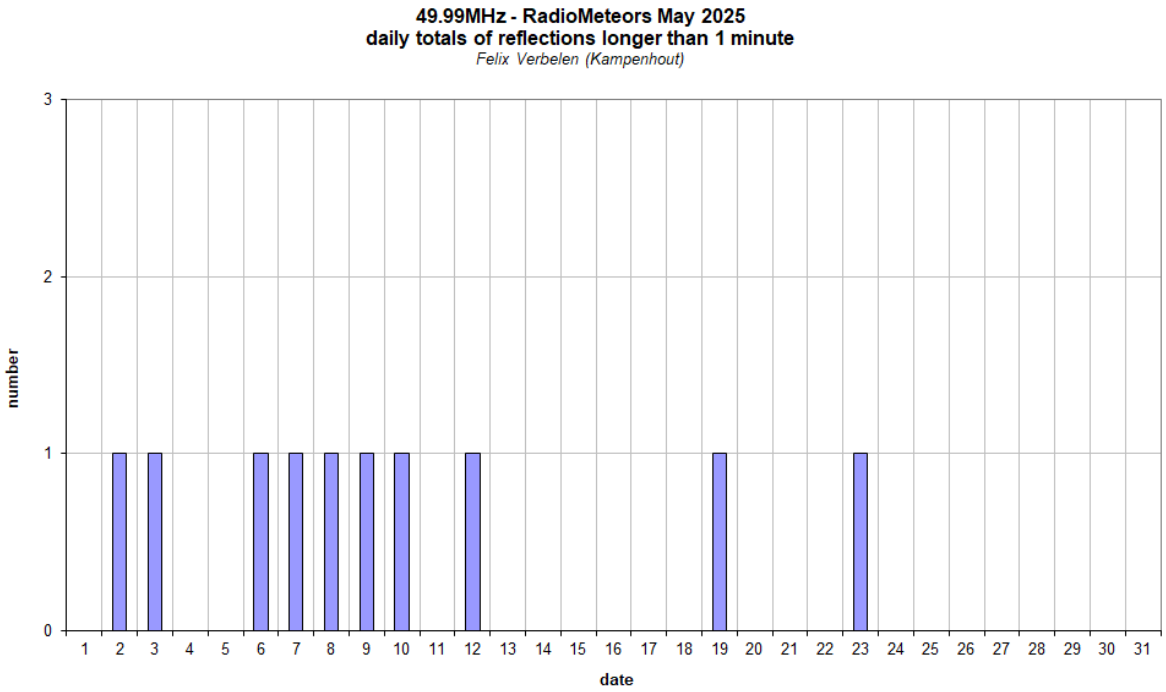

Figure 2 – The daily totals of overdense reflections longer than 10 seconds and longer than 1 minute, as observed here at Kampenhout (BE) on the frequency of our VVS-beacon (49.99 MHz) during May 2025.

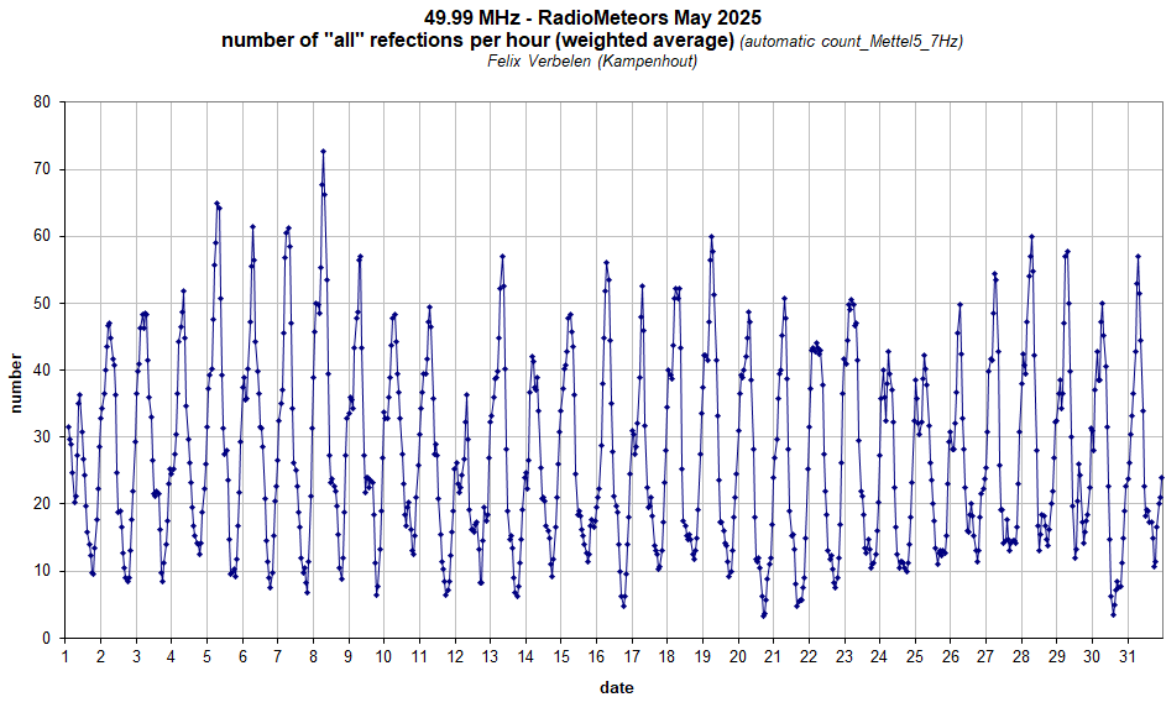

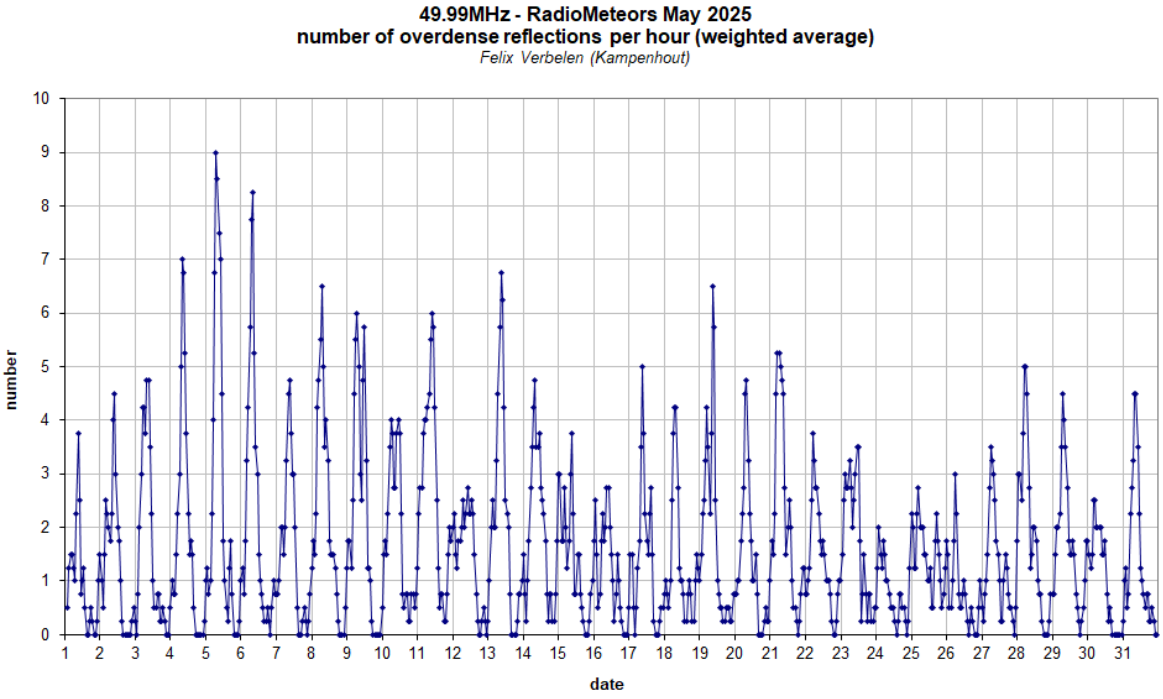

Figure 3 – The hourly numbers of "all" reflections counted automatically, and of manually counted "overdense" reflections, as observed here at Kampenhout (BE) on the frequency of our VVS-beacon (49.99 MHz) during May 2025.

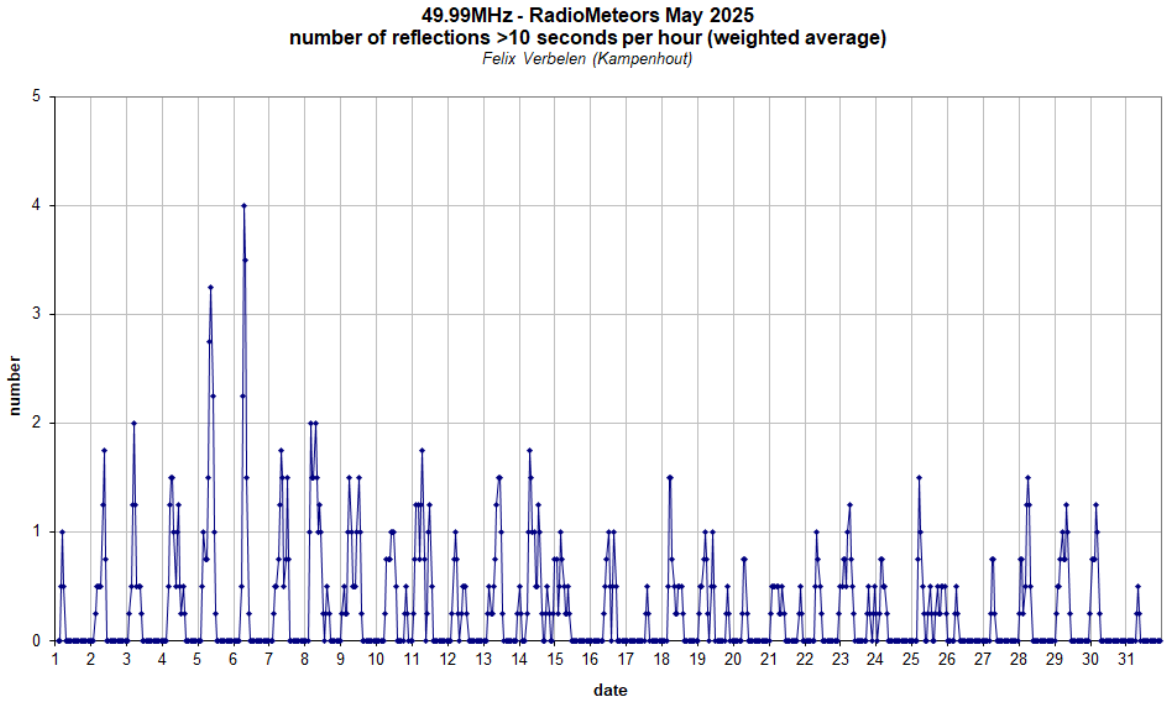

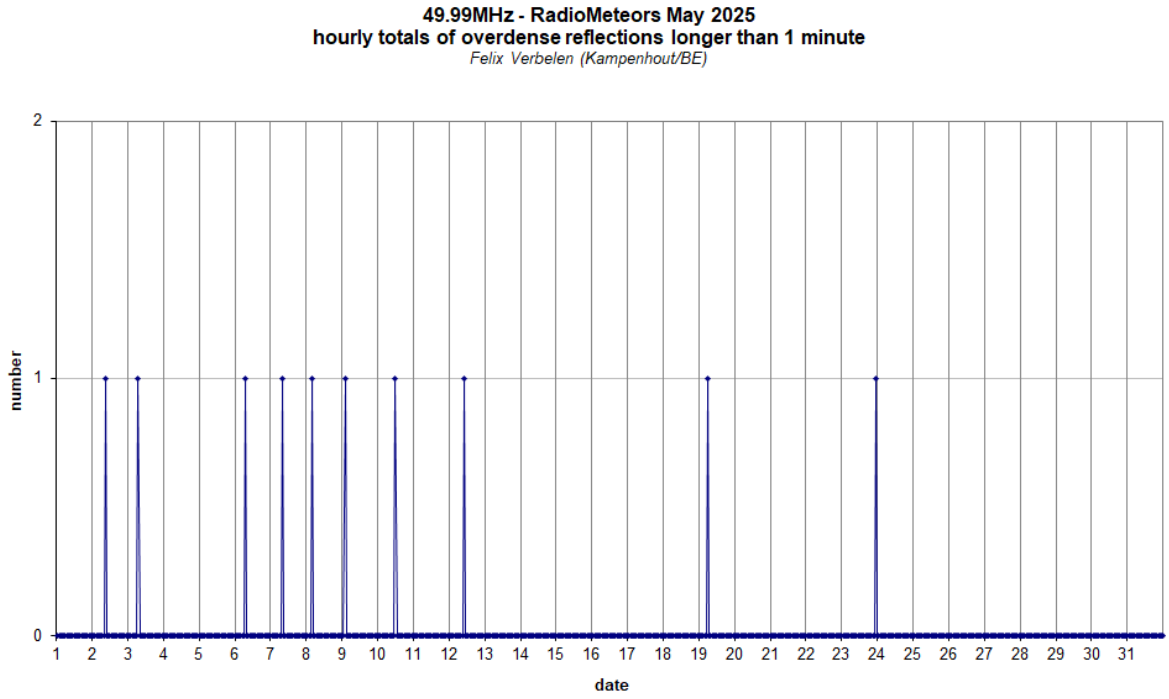

Figure 4 – The hourly numbers of overdense reflections longer than 10 seconds and longer than 1 minute, as observed here at Kampenhout (BE) on the frequency of our VVS-beacon (49.99 MHz) during May 2025.

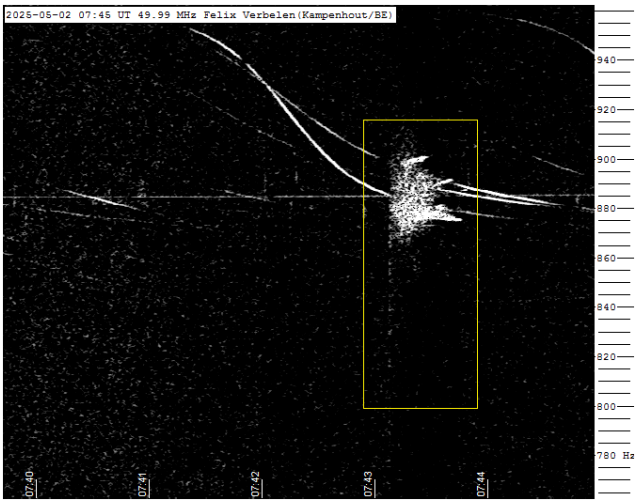

Figure 5 – Meteor echoes May 2, 7^h45^m UT.

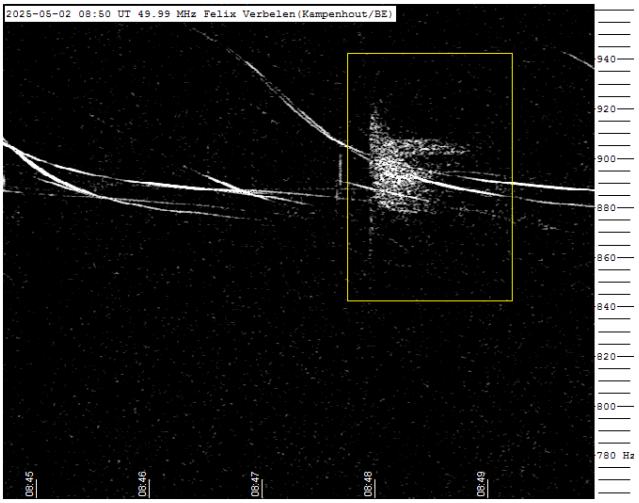

Figure 6 – Meteor echoes May 2, 8^h50^m UT.

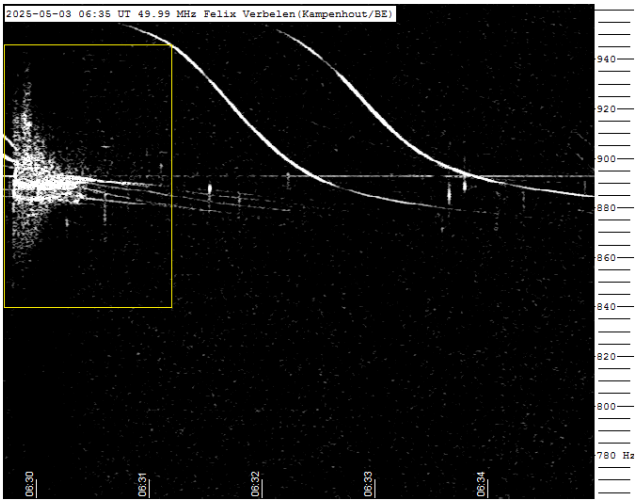

Figure 7 – Meteor echoes May 3, 6^h35^m UT.

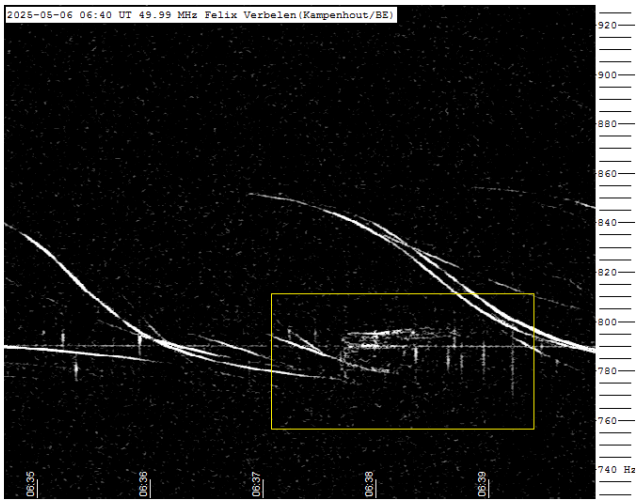

Figure 8 – Meteor echoes May 6, 6^h40^m UT.

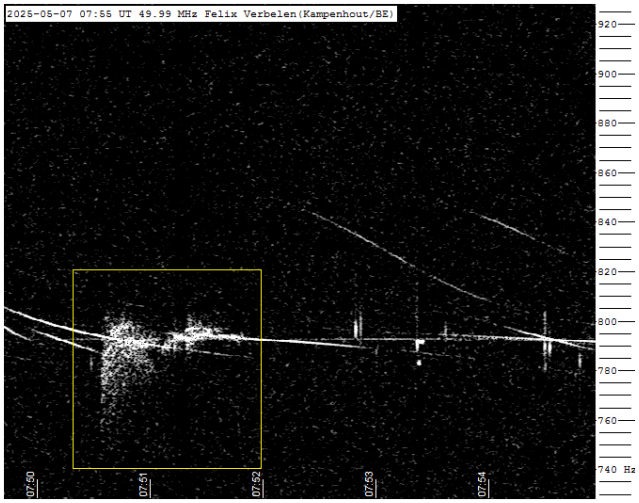

Figure 9 – Meteor echoes May 7, 7^h55^m UT.

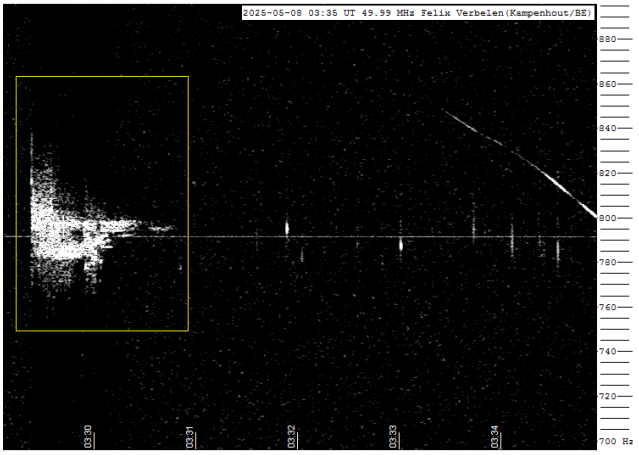

Figure 10 – Meteor echoes May 8, 3^h35^m UT.

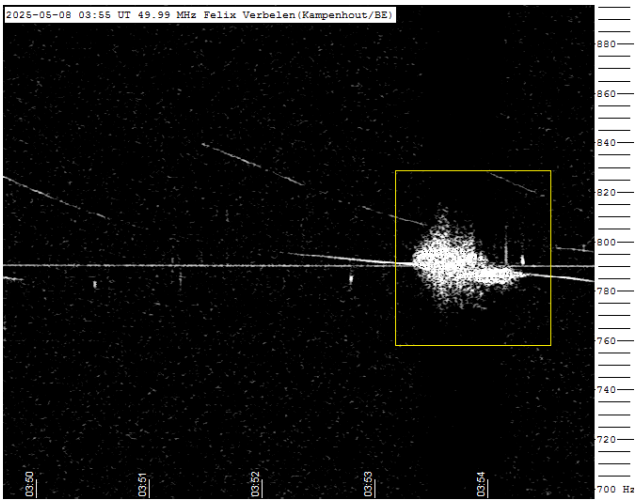

Figure 11 – Meteor echoes May 8, 3^h55^m UT.

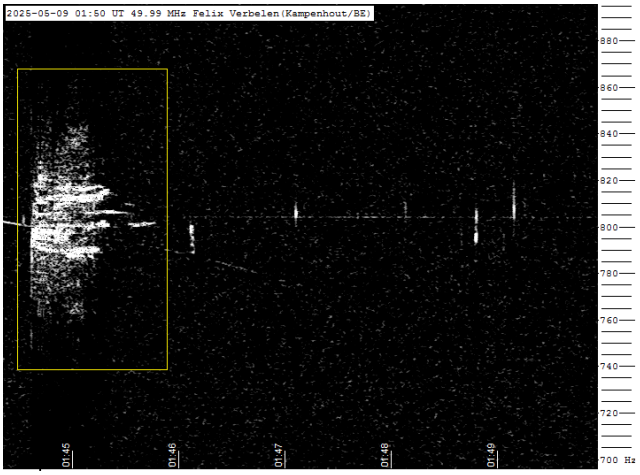

Figure 12 – Meteor echoes May 9, 1^h50^m UT.

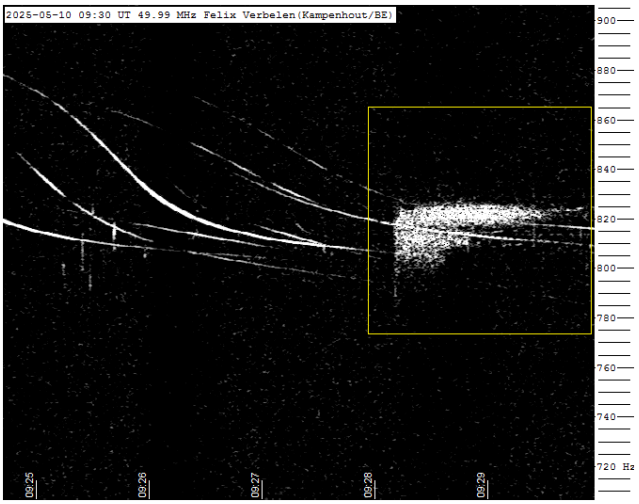

Figure 13 – Meteor echoes May 10, 9^h30^m UT.

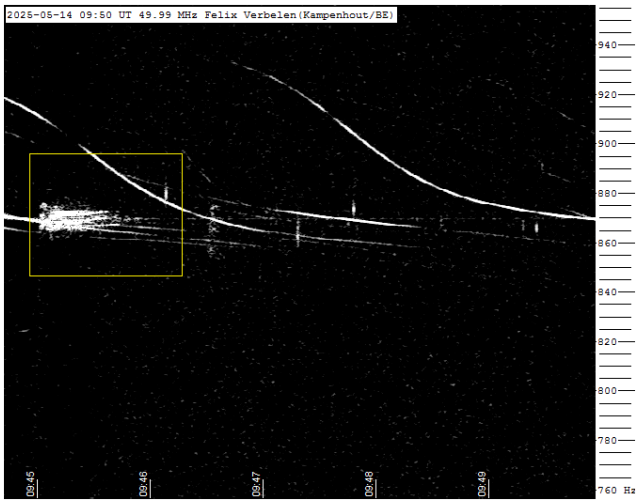

Figure 14 – Meteor echoes May 14, 9^h50^m UT.

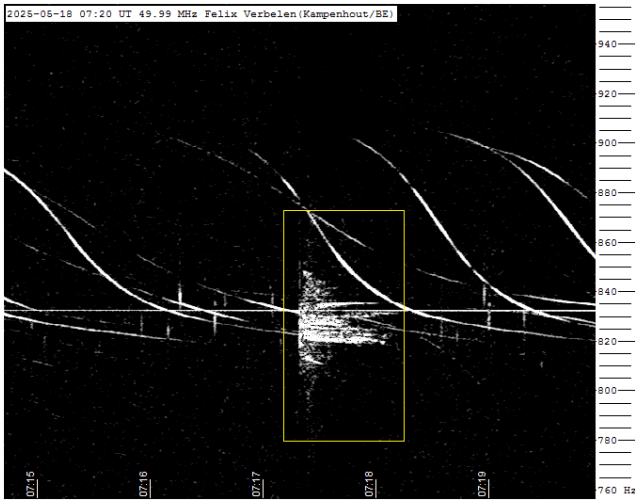

Figure 15 – Meteor echoes May 18, 7^h20^m UT.

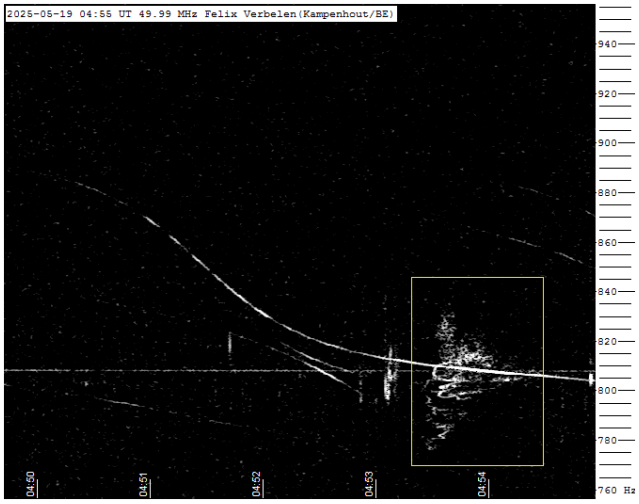

Figure 16 – Meteor echoes May 19, 4^h55^m UT.

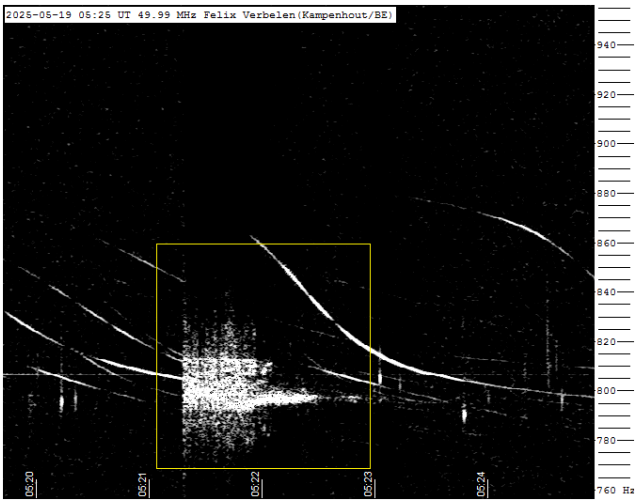

Figure 17 – Meteor echoes May 19, $5^{h}25^{m}$ UT.

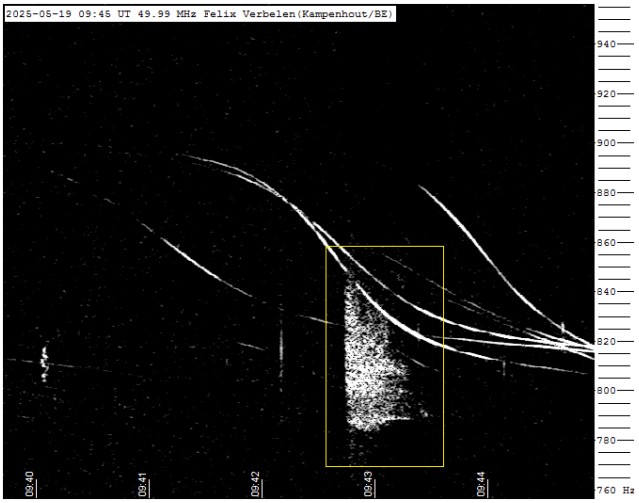

Figure 18 – Meteor echoes May 19, $9^{h}45^{m}$ UT.

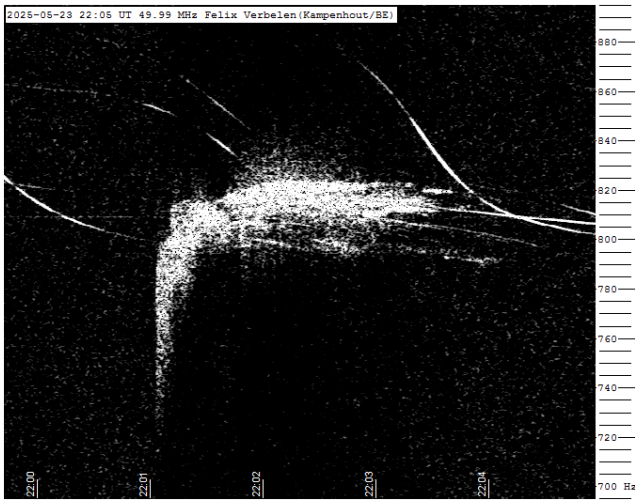

Figure 19 – Meteor echoes May 23, $22^{h}05^{m}$ UT.

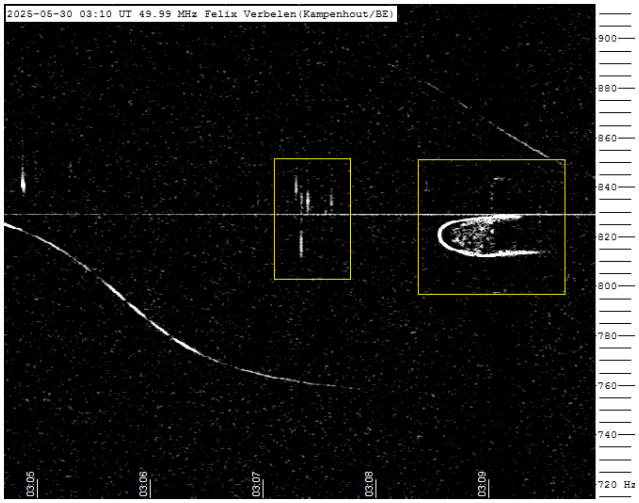

Figure 20 – Meteor echoes May 30, $3^{h}10^{m}$ UT.

eMetN METEOR JOURNAL

Since 2016 the mission of eMetN Meteor Journal is to offer meteor news to a global audience and to provide a swift exchange of information in all fields of active amateur meteor work. eMetN Meteor Journal is freely available without any fees. eMetN Meteor Journal is independent from any country, society, observatory or institute. Articles are abstracted and archived with ADS Abstract Service: https://ui.adsabs.harvard.edu/search/q=eMetN

You are welcome to contribute to eMetN Meteor Journal on a regular or casual basis, if you wish to. Anyone can become an author or editor, for more info read: https://www.emeteornews.net/writing-content-for-emeteornews/

Articles for eMetN Meteor Journal should be submitted to: paul.roggemans@gmail.com

Contact: info@emeteornews.net

Contributors:

- Barbieri L.
- Campbell-Burns P.
- Jakubík M.
- Maglione M.
- Miskotte K.
- Neslušan L.
- Roggemans P.
- Sarto S.
- Šegon D.
- Sekiguchi T.
- Verbelen F.
- Vida D.

Online publication https://www.emeteornews.net and https://www.emetn.net
ISSN 3041-4261, publisher: Paul Roggemans, Pijnboomstraat 25, 2800 Mechelen, Belgium